Journal of Superconductivity and Novel Magnetism
https://doi.org/10.1007/s10948-024-06808-4

RESEARCH

Investigation of Gamma-Induced Changes to Screening Currents and AC Losses in Mono- Versus Multi-filamentary REBCO Coated Conductors Using DC and AC Magnetometry

Holly Jane Campbell[1] · Hirokazu Sasaki[2] · Yifei Zhang[3]

Received: 15 May 2024 / Accepted: 16 July 2024

Abstract
REBCO (rare-earth barium copper oxide) coated conductor tapes are a highly attractive option for magnet materials in future tokamak fusion power plants. However, the threat of intense neutron and gamma radiation, together with AC losses during magnet coil ramping, has raised concerns around magnet coil lifetimes. Irradiation-induced changes to flux creep rate has been identified as a key performance-limiting factor in REBCO tapes at low temperatures and high fields post-irradiation with gamma rays; spontaneous flux creep contributes to hysteretic AC loss in REBCO cables under applied AC fields. Knowing that multi-filamentary tapes are under consideration for tokamaks as an AC loss mitigation, magnetic measurements and gamma irradiation experiments are presented here on striated and mono-filamentary YBCO tapes to investigate the differences in post-irradiation screening currents and AC losses. Reduction in AC losses improved magnetisation critical current density (J_c) retention after 1 MGy in the multi- relative to the mono-filamentary samples. After the 5 MGy dose, striations then made the multi-filamentary tape more susceptible to J_c degradation because of the thinner individual filament width. Scanning transmission electron microscopy analysis on an analogous GdYBCO mono-filamentary tape did not indicate the introduction of nm-scale amorphisation to the active GdYBCO layer after gamma irradiation. A potential theoretical explanation for the underlying mechanism altering the flux-pinning landscape across the REBCO layer surface in gamma-irradiated tapes is discussed. This work concluded that gamma effects on screening current capability should be considered in future tokamak REBCO tape qualification studies.

Keywords REBCO · Coated conductors · Fusion magnets · Gamma irradiation · AC losses

1 Introduction

Future fusion power plants intend to use REBCO (rare-earth barium copper oxide) coated conductor tapes as the tokamak magnet material because of their high critical temperatures (T_c), magnetic fields (B_c), and current densities (J_c) [1]. In tokamaks, REBCO tapes must carry high transport currents under high fields [2], and particularly during magnet coil current ramping, prevention of power dissipation through mitigation of AC loss is desirable [3, 4]. Striated, multi-filamentary REBCO tape has been suggested as a potential AC loss mitigation strategy because reduction of the filament cross-sectional area minimises magnetisation screening current effects in individual tapes [5–9]. Irradiation-induced changes to flux creep rate was identified in our previous study as a major performance-limiting factor in standard, mono-filamentary REBCO tape under tokamak-relevant fields and temperatures [10]. In REBCO cables under applied AC fields, hysteretic AC loss occurs because magnetic flux quanta must rearrange themselves in order to follow the time-varying excitation; this flux quanta motion leads to voltage build up and dissipation of energy from the supercurrent due to Faraday's Law. Spontaneous flux creep contributes to hysteretic loss [11]. Therefore, the aim of this study was to investigate post-irradiation changes to screening currents and AC losses in

✉ Holly Jane Campbell
holly.campbell@ukaea.uk

[1] UKAEA (United Kingdom Atomic Energy Authority), Culham Campus, Abingdon, Oxfordshire OX14 3DB, UK

[2] Furukawa Electric Co. Ltd, 2-4-3, Okano, Nishi-Ku, Yokohama 220-0073, Japan

[3] SuperPower Inc, 21 Airport Road, Glenville, NY 12302, USA

Published online: 05 August 2024

mono- versus multi-filamentary YBCO tapes. The anticipated outcome was that striations would lower post-irradiation AC loss, thus improving retention of J_c in REBCO tapes and potential magnet coil lifetimes.

Gamma rays are expected to bombard tokamak magnets [12], but literature on the effects of gamma irradiation on REBCO remains inconsistent and contradictory. Co-60 irradiation studies on YBCO thick films and EuBCO bulk samples suggested that gamma rays reduce T_c and J_c by introducing crystal lattice disorder in the form of oxygen Frenkel pairs [13, 14]. Other studies on bulk YBCO and ErBCO showed no evidence of introduced microstructural damage, though were indicative of gamma-induced changes to the REBCO electronic structure [15, 16]. Electrical testing on coated conductor tapes during and after low doses of gamma radiation did not demonstrate T_c or J_c degradation in two recent studies [17, 18]. However, in our previous study, magnetic testing on coated conductor tape samples after a 1 MGy gamma dose revealed significant changes to T_c, J_c, and flux creep rate, which were dependent on the pristine flux-pinning landscape and the presence/absence of the Cu stabiliser [10].

Electrical and magnetic measurements provide information on different functional parameters in superconductors: whilst electrical testing probes the bulk transport currents, magnetometry probes the surface magnetisation (screening) currents [19]. One of the conclusions from magnetic analysis in [10] was that gamma rays alter the flux-pinning landscape in REBCO tapes, despite gamma irradiation having no effect on transport currents in [17] and [18]. In [10], the microscopic origin of the resulting gamma effects was not proposed nor investigated.

In this work, magnetic testing before and after gamma irradiation comprised of DC moment versus field hysteresis loop and AC susceptibility measurements for calculation of magnetisation-J_c and AC loss, respectively. STEM analysis on an analogous GdYBCO tape examined in our previous study [10] is included with reference to the associated magnetometry data because it inspired the proposed theoretical origin of gamma effects on REBCO tapes discussed in this work.

Post-irradiation changes to J_c and AC loss in the mono- and multi-filamentary tape samples are evaluated. This magnetic analysis expands on the understanding of gamma-induced flux-pinning landscape evolution explored in our previous study [10] by incorporating connections between observed data and changes in the London penetration depth and coherence length parameters described by Ginzburg–Landau theory.

2 Methods

2.1 Samples and Irradiation

The tapes assessed in this work were 2 analogous mono-/multi-filamentary SuperPower 4 mm wide SCS4050 YBCO samples (Fig. 1). Both tapes had 15% Zr doping within the YBCO layer to form $BaZrO_3$ nanocolumns to act as artificial pinning centres (APC). Furukawa Electric Co., Ltd and SuperPower Inc. developed the multi-filamentary tape together, using a laser to introduce 3 striation lines along the length of the tape, resulting in a YBCO layer composed of 4×1 mm wide filaments [20, 21].

For all measurements, 3 mm disk samples were cut from the tapes prior to irradiation using a SPI Supplies #17,001-AB precision TEM disk punch. All multi-filamentary disks were cut such that the 3 striation lines would be present for irradiation/analysis; the disk samples would therefore contain the full width of the 2 middle filaments and partial widths of the 2 outer filaments.

Gamma irradiation experiments were carried out at the Dalton Cumbrian Facility. The YBCO tape samples were irradiated with Co-60 gamma rays to 1 and 5 MGy doses. The energies of Co-60 gamma rays (1.17 and 1.33 MeV) are expected to be within the appropriate energy range of

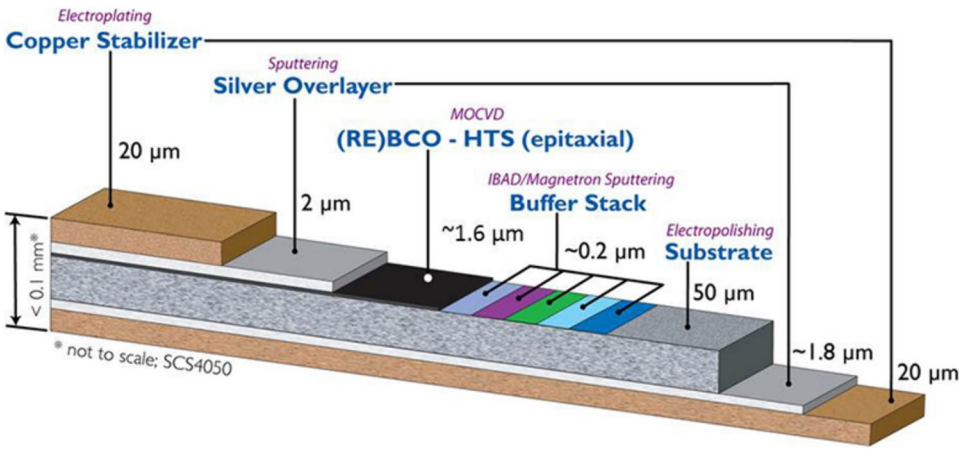

Fig. 1 Schematic diagram of a SuperPower SCS4050 REBCO coated conductor tape [22]

emitted gamma rays from the fusion plasma, and a dose of 1 MGy is estimated to bombard the magnets in spherical tokamaks after ~ 60 days [12]. In our previous study [10], the GdYBCO tape samples were also irradiated to a 1 MGy dose; this allowed a direct comparison of 1 MGy gamma irradiation effects on analogous YBCO and GdYBCO samples. The 5 MGy dose was then chosen to enable evaluation of prolonged gamma irradiation effects.

During gamma irradiation experiments, the mono-filamentary and multi-filamentary repeat samples, each numbered 1, 2 and 3, were in the same horizontal position on the sample holder, i.e. both repeat sample number 2 disks were in the centre of the sample holder, with the mono-filamentary sample 2 a few mm directly above the multi-filamentary sample 2.

The irradiation angle was parallel to the YBCO *c*-axis. It is assumed that gamma irradiation effects are isotropic, thus the angle of irradiation does not influence changes in functionality [10, 23].

2.2 Measurement Setup

Magnetometry measurements were conducted on the YBCO tape disk samples using the AC magnetic susceptibility (ACMS) operational mode of a Quantum Design PPMS® DynaCool™ Physical Property Measurement System (PPMS). For all measurements, magnetic fields were applied parallel to the YBCO *c*-axis. During AC susceptibility measurements, a 0.001 T AC drive field with a frequency of 777 Hz was also applied along with the DC field.

Each disk sample was measured before and after irradiation. For both radiation doses, 3 repeat samples from each tape were cut: in total, 6 samples from the mono-filamentary tape and 6 samples from the multi-filamentary tape were irradiated (3 samples to 1 MGy and 3 samples to 5 MGy, respectively). Due to striations reducing achievable J_c in multi-filamentary tapes as a consequence of the removed YBCO material, determination of radiation tolerance in comparison to the mono-filamentary tape focussed on relative changes post-irradiation and not absolute values. Measurements on the same samples pre-/post-irradiation and on repeat samples reinforced confidence in the observed functionality changes.

Scanning transmission electron microscopy (STEM) imaging was conducted on analogous mono-filamentary SuperPower 4 mm wide SCS4050 GdYBCO tape samples. The pre-/post-irradiation samples contained 15% Zr doping within the GdYBCO layer for APC generation, and the Cu stabiliser was chemically etched off the tape section prior to disk punching and irradiation. The 15% Zr Ag-only samples were observed using STEM before/after Co-60 gamma irradiation to a dose of 1 MGy. The corresponding magnetometry measurement analysis was previously discussed in [10]. ACMS mode PPMS measurements on the aforementioned GdYBCO tape samples applied the same experimental parameters as used in measurements on the YBCO tape samples presented in this work.

STEM samples were prepared using the focussed ion beam (FIB) method from 3 mm disks. A Seiko Instruments SMI3050TB was used for FIB fabrication with a Ga^+ ion beam acceleration voltage of 30 kV. A 2-kV Ar ion milling process was applied for 5 min to remove the damaged layer formed by FIB. A JEOL-ARM equipped with a STEM Cs-corrector was used for high-angle annular dark field (HAADF) STEM observation along the *ab*-axis direction at an acceleration voltage of 200 kV.

2.3 Data Analysis Calculations

Values for magnetisation-J_c were calculated from DC magnetic moment versus applied magnetic field hysteresis loops (an example hysteresis loop is shown in Fig. 2) using Bean's critical state model for a thin film: $J_c = (15\Delta m)/(Vr)$, where Δm is the magnetic moment difference, V is REBCO layer volume and r is the sample radius [24, 25].

Values for AC losses were calculated from the maximum value of imaginary susceptibility (χ'') in AC susceptibility measurements using the following equation: AC loss $= (V\pi\chi'')(B_{max}^2/\mu_0)$, where B_{max} is the AC drive field and μ_0 is the permeability of free space (an example susceptibility profile is shown in Fig. 3) [26].

REBCO layer volume was treated as a constant value across disk samples during analysis of all mono- and multi-filamentary samples, respectively.

3 Results and Discussion

3.1 Magnetisation Critical Current Density

3.1.1 YBCO Mono-filamentary Tape

Figures 4 and 5 show the calculated J_c values for the mono-filamentary samples versus field, pre-irradiation and after 1 and 5 MGy gamma doses, respectively. Figures 6 and 7 contain the calculated percentage changes in J_c for the same samples post-irradiation.

After irradiation to both doses, J_c decreased across all measured field strengths. On average, there was less J_c degradation after 5 MGy. From previous work, lessening of J_c degradation was assumed to be attributed to the reduction of AC loss with increasing gamma dose (theory discussed fully in Sect. 3.3.1) [10]. Decreases in J_c were consistent within a couple of percent in all 3 repeat samples after 1 MGy, but after 5 MGy the change in J_c varied: in 2 of the 5 MGy irradiated repeat samples, the decrease in J_c was smaller than

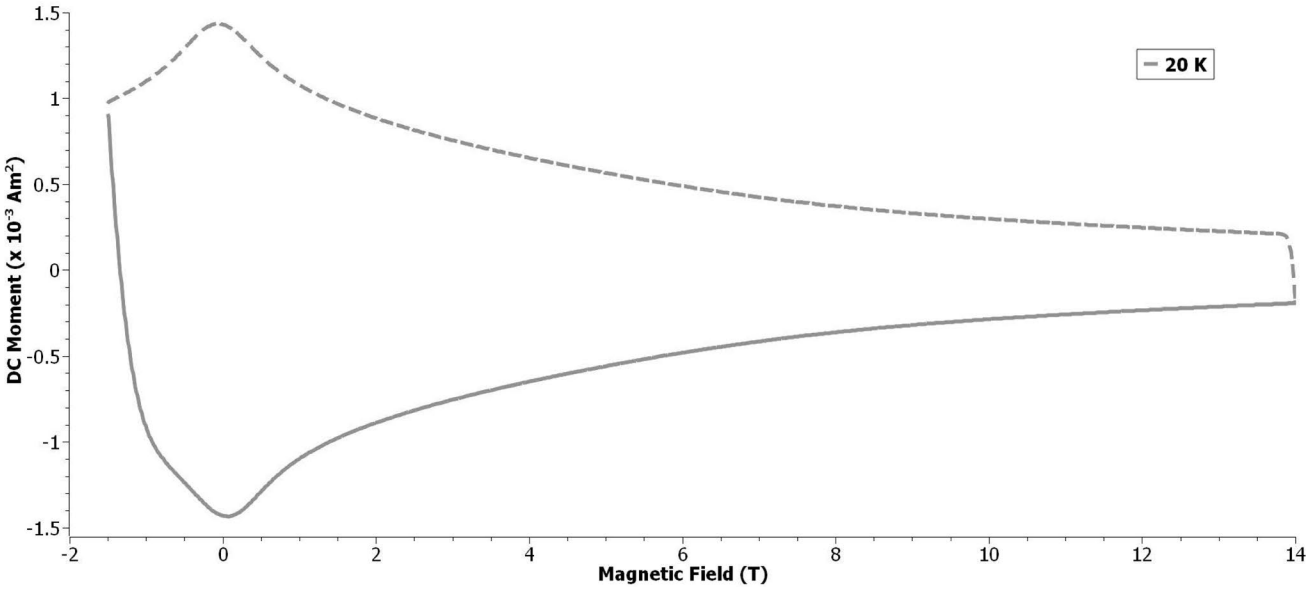

Fig. 2 DC magnetic moment versus magnetic field hysteresis loop for a mono-filamentary tape sample prior to gamma irradiation – J_c values were calculated from hysteresis loops measured at 20 K

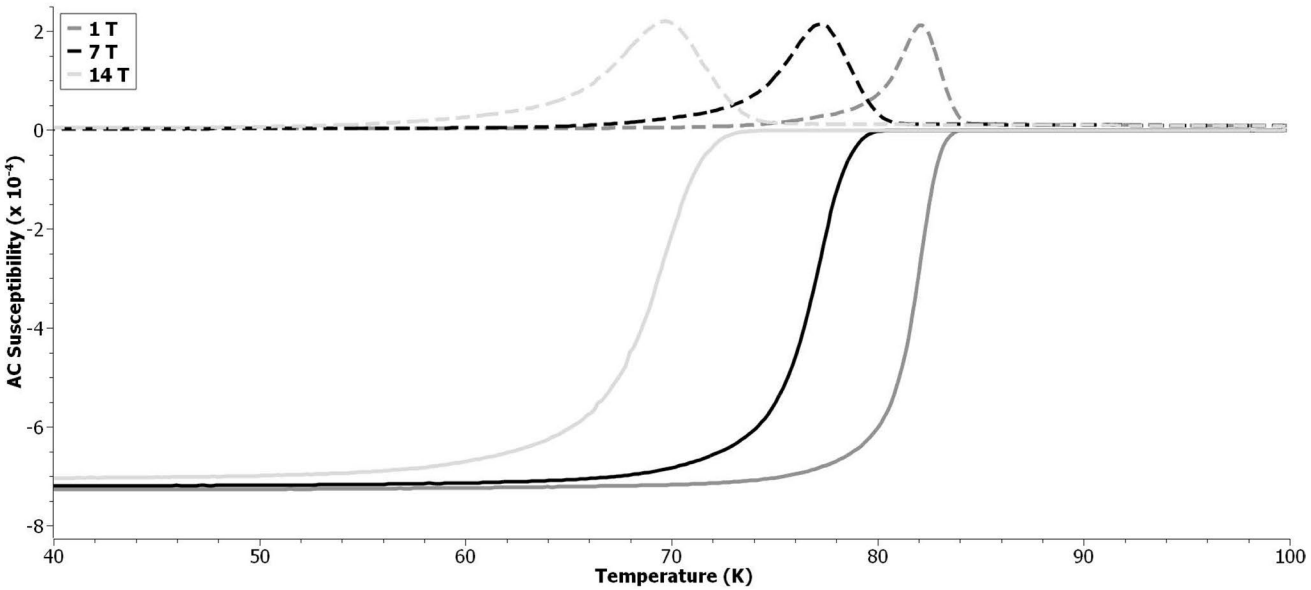

Fig. 3 AC susceptibility versus temperature for a mono-filamentary tape sample prior to gamma irradiation—susceptibility values at 1, 7 and 14 T

the 1 MGy sample mean, but in the third repeat sample, the decrease in J_c was larger.

Due to the inconsistency in J_c degradation after irradiation to 5 MGy across the repeat samples (large error associated with mean value), objective claims relating to radiation tolerance or post-irradiation mean parameter values could not be made, and it is acknowledged that further study into prolonged gamma irradiation effects using a greater sample size is necessary.

However, the data collected on the 5 MGy irradiated samples remained valuable, providing additional insight into the connections between post-irradiation magnetic property parameter changes, i.e., the connections between AC losses, superconducting volume fraction and J_c. These connections are discussed in detail in Sect. 3.3.

It was also noted that the observed post-irradiation percentage decreases in J_c were very minor; this is expanded on in Sect. 3.1.2.

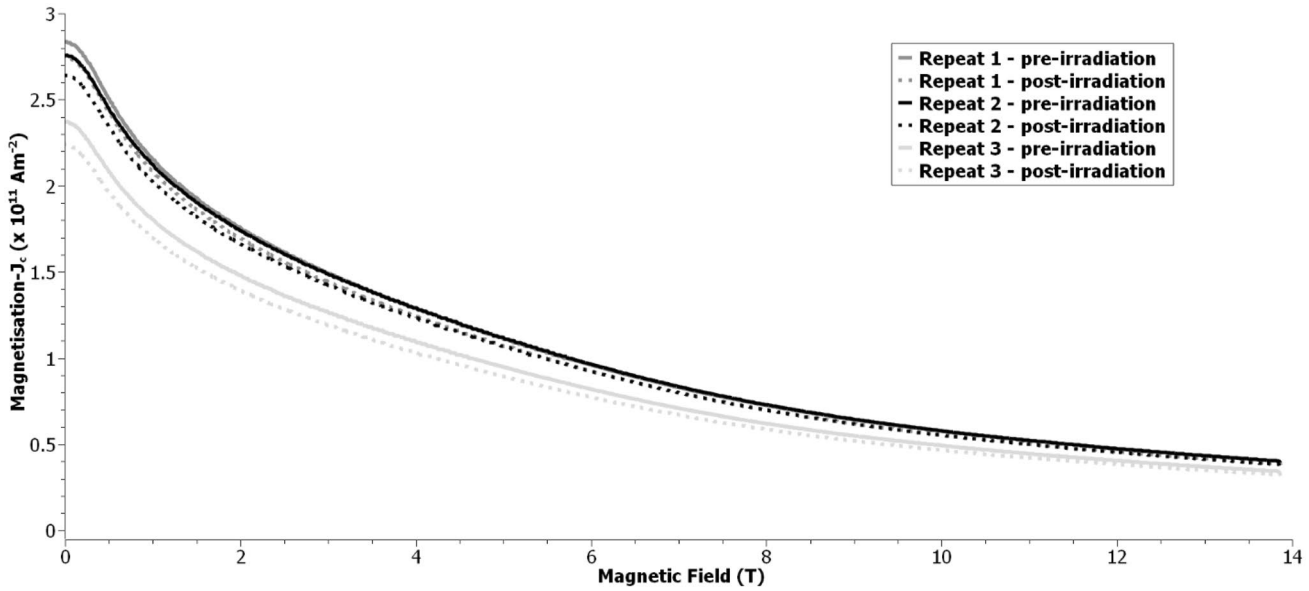

Fig. 4 Magnetisation critical current density versus magnetic field for the mono-filamentary repeat samples prior to and post 1 MGy gamma irradiation – J_c values calculated at 20 K

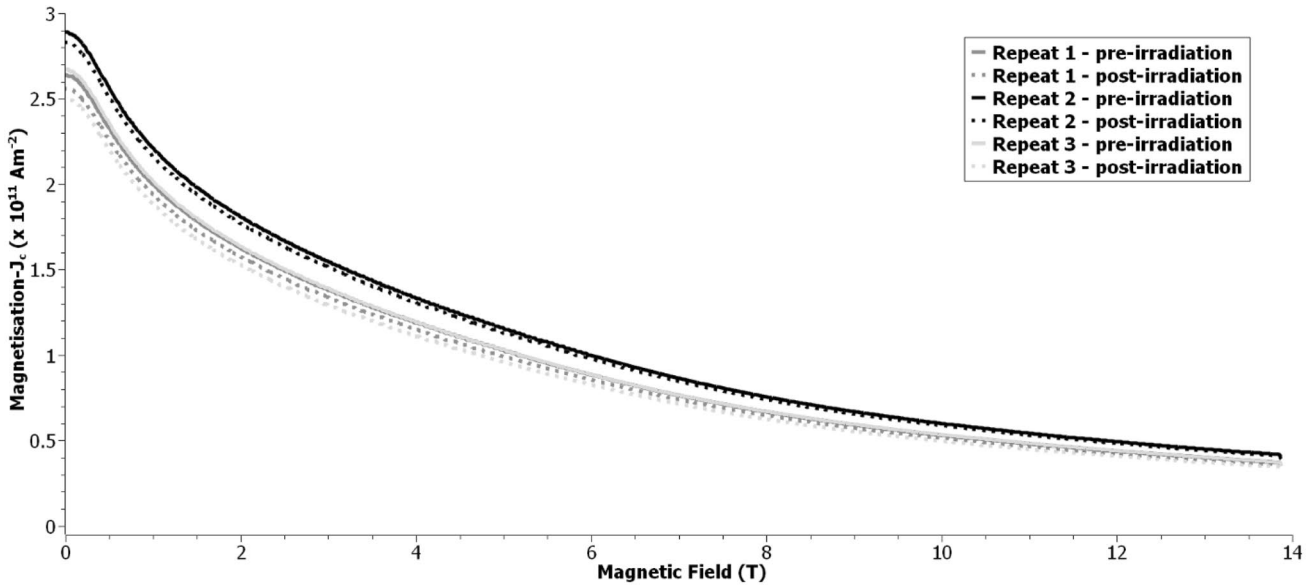

Fig. 5 Magnetisation critical current density versus magnetic field for the mono-filamentary repeat samples prior to and post 5 MGy gamma irradiation – J_c values calculated at 20 K

3.1.2 YBCO Multi-filamentary Tape

Figures 8 and 9 show the calculated J_c values for the multi-filamentary samples versus field, pre-irradiation and after 1 and 5 MGy gamma doses, respectively. Figures 10 and 11 contain the calculated percentage changes in J_c for the same samples post-irradiation.

As seen in the analogous mono-filamentary samples, J_c decreased across all measured field strengths post-irradiation with both gamma doses in the multi-filamentary samples. On average, J_c degradation was greater after 5 MGy. Decreases in J_c were consistent in all 3 repeat samples after 1 MGy, but after 5 MGy the degree of J_c degradation fluctuated: in the 5 MGy irradiated repeat samples 2 and 3, the decrease

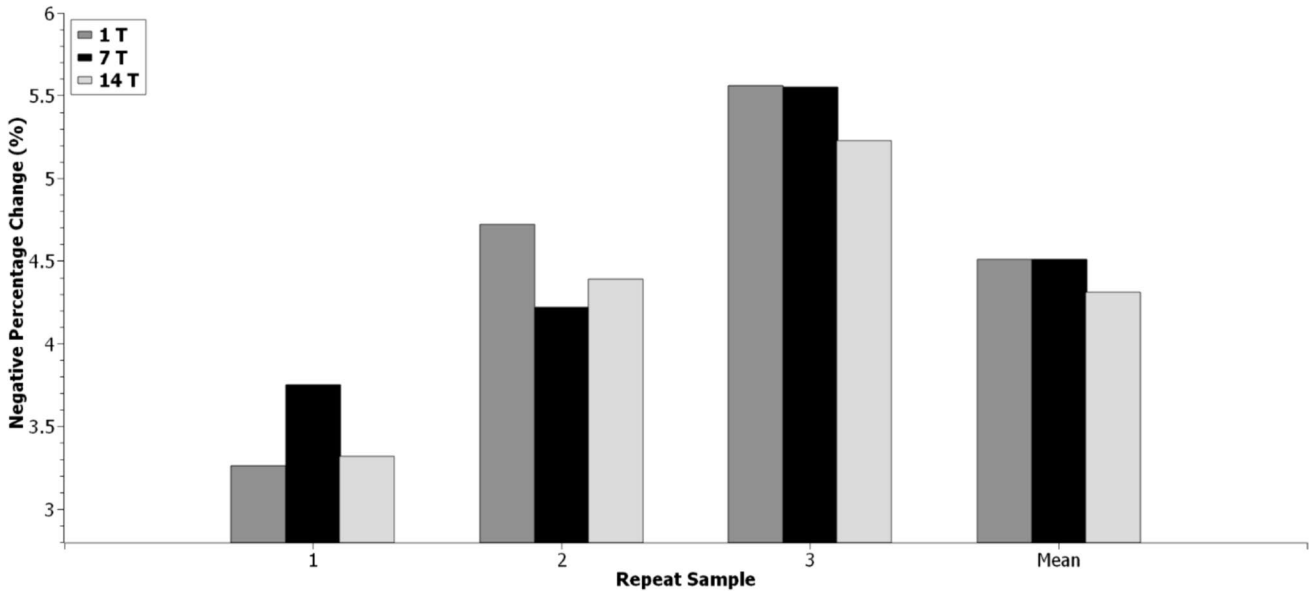

Fig. 6 Percentage change in magnetisation critical current density at 1, 7 and 14 T for the mono-filamentary repeat samples post 1 MGy gamma irradiation – J_c values calculated at 20 K

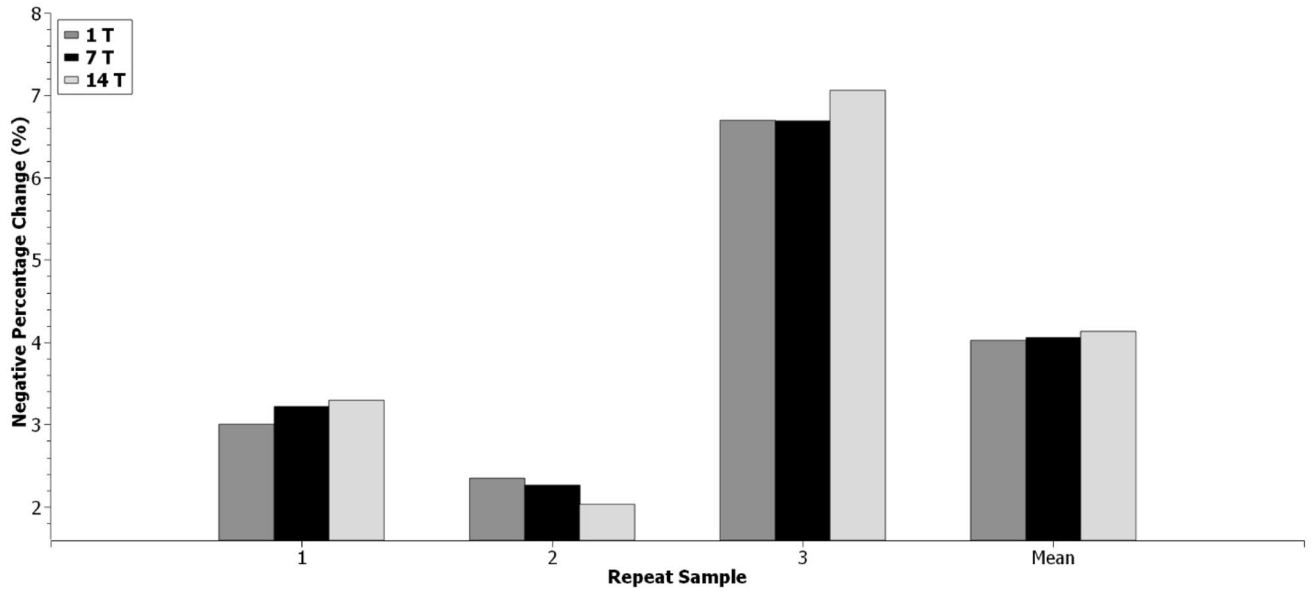

Fig. 7 Percentage change in magnetisation critical current density at 1, 7 and 14 T for the mono-filamentary repeat samples post 5 MGy gamma irradiation – J_c values calculated at 20 K

in J_c was larger than the 1 MGy sample mean, but in the first repeat sample, the decrease in J_c was smaller.

Comparing the mono- and multi-filamentary samples (Fig. 12), after 1 MGy the multi-filamentary samples displayed better retention of high J_c. Objective assessment of radiation tolerance in the mono- versus multi-filamentary samples after 5 MGy irradiation was not possible due to the inconsistencies in J_c degradation across the repeat samples; however, a pattern in post-irradiation functionality changes was acknowledged. Increasing the gamma dose to 5 MGy resulted in greater mean percentage reduction of J_c thus lower relative mean post-irradiation J_c values in the multi-filamentary samples.

Although the percentage decrease in J_c post-irradiation to 5 MGy varied across repeats in each sample set, a distinct trend was observed when comparing these values to the percentage decreases in J_c after 1 MGy irradiation: mono-filamentary samples tended towards improvement in J_c retention

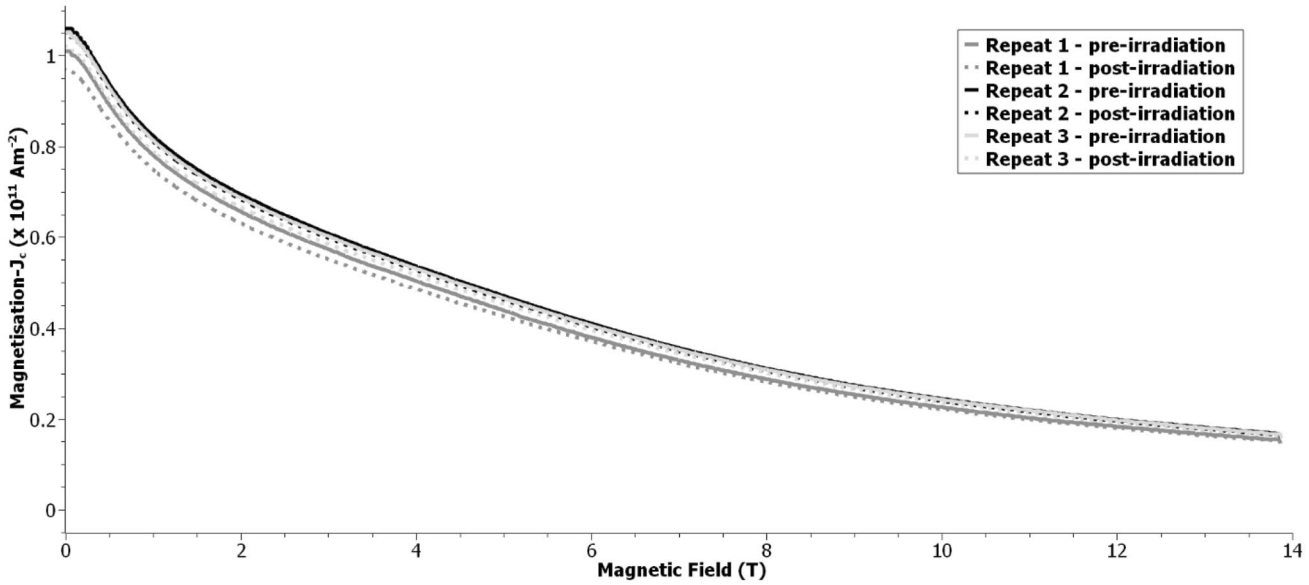

Fig. 8 Magnetisation critical current density versus magnetic field for the multi-filamentary repeat samples prior to and post 1 MGy gamma irradiation – J_c values calculated at 20 K

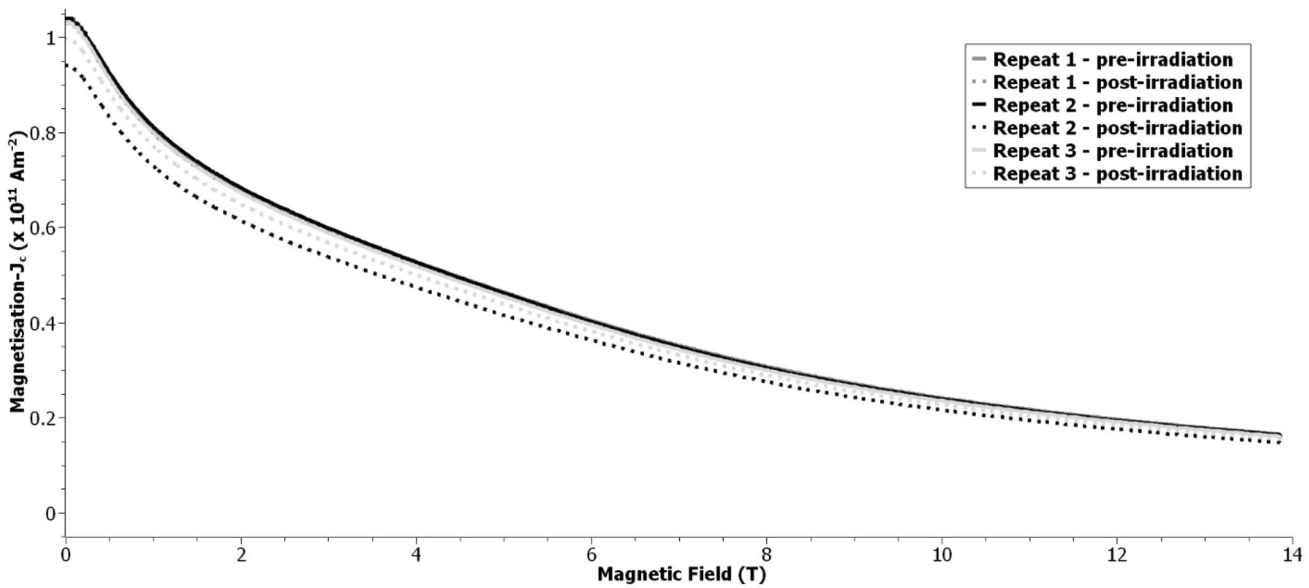

Fig. 9 Magnetisation critical current density versus magnetic field for the multi-filamentary repeat samples prior to and post 5 MGy gamma irradiation – J_c values calculated at 20 K

when dose increased from 1 to 5 MGy, whilst the multi-filamentary samples tended towards greater reduction in J_c.

After 5 MGy irradiation, the pattern in J_c percentage decreases discussed above did not correspond to the same repeat sample number in each sample set, and therefore not to the same horizontal position on the sample holder, e.g., the largest decreases in J_c were observed in the mono-filamentary repeat sample 3 and multi-filamentary repeat sample 2. This indicated that the differences in J_c after 5 MGy irradiation were not caused by an experimental setup error.

In both the mono- and multi-filamentary samples, the decrease in J_c was minor even after irradiation to the high 5 MGy dose. After ACMS measurements and irradiation, there was no visible damage to the disk sample edges. A concern was that the 'gamma-induced, post-irradiation

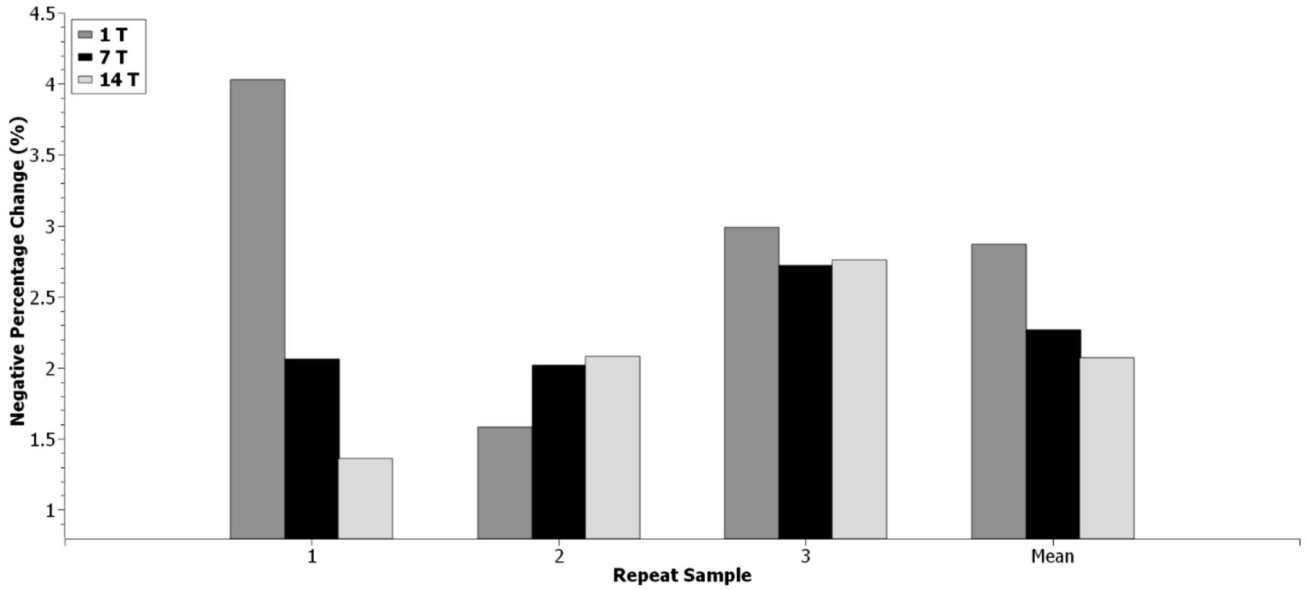

Fig. 10 Percentage change in magnetisation critical current density at 1, 7 and 14 T for the multi-filamentary repeat samples post 1 MGy gamma irradiation – J_c values calculated at 20 K

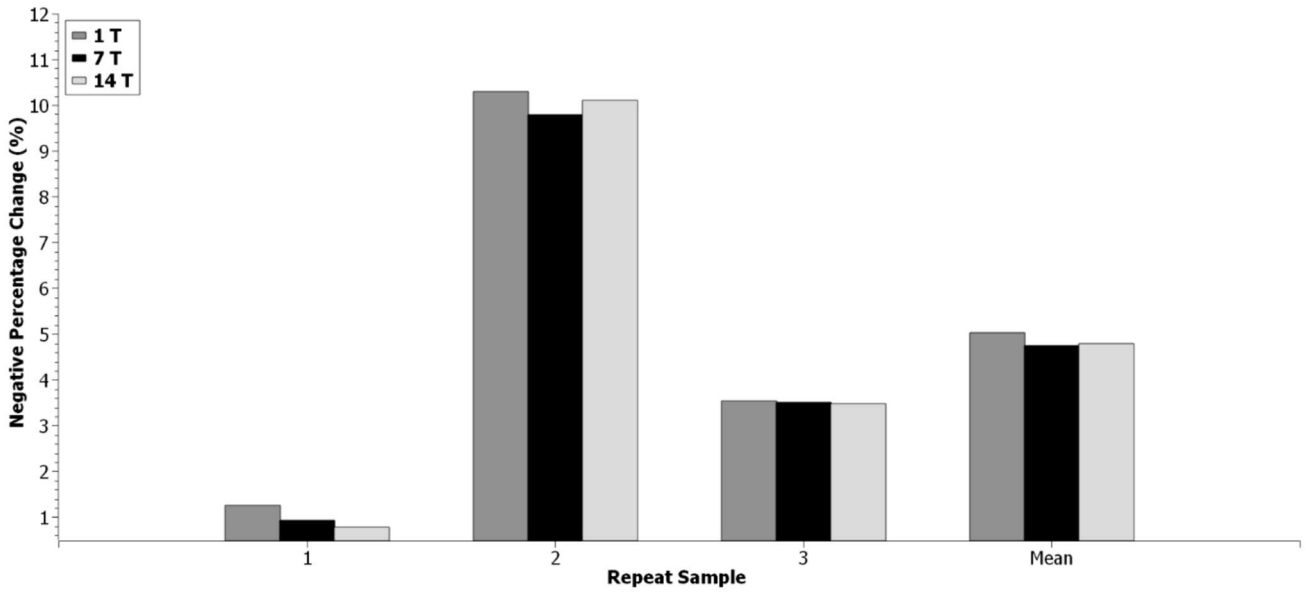

Fig. 11 Percentage change in magnetisation critical current density at 1, 7 and 14 T for the multi-filamentary repeat samples post 5 MGy gamma irradiation – J_c values calculated at 20 K

functionality changes' explored in this work and in [10] could instead have been a result of REBCO aging effects.

In a study by Schlesier et al., over the course of 5 months J_c decreased with time in YBCO and GdBCO thin-films due to sample aging caused by out-diffusion of oxygen; T_c also decreased with time in the Au-coated GdBCO sample [27]. However, there was no observable reduction in diamagnetic saturation with time in YBCO or GdBCO, nor did the pinning structure change over the 5-month period [27].

Both campaigns of pre-/post-irradiation testing and irradiation experiments on the YBCO and GdYBCO samples investigated in this work were completed within a similar timeframe of around 5 months. Therefore, whilst aging may have contributed to post-irradiation J_c and T_c degradation in the YBCO and GdYBCO samples, aging effects do not account for the post-irradiation changes in superconducting volume fraction nor pinning landscape.

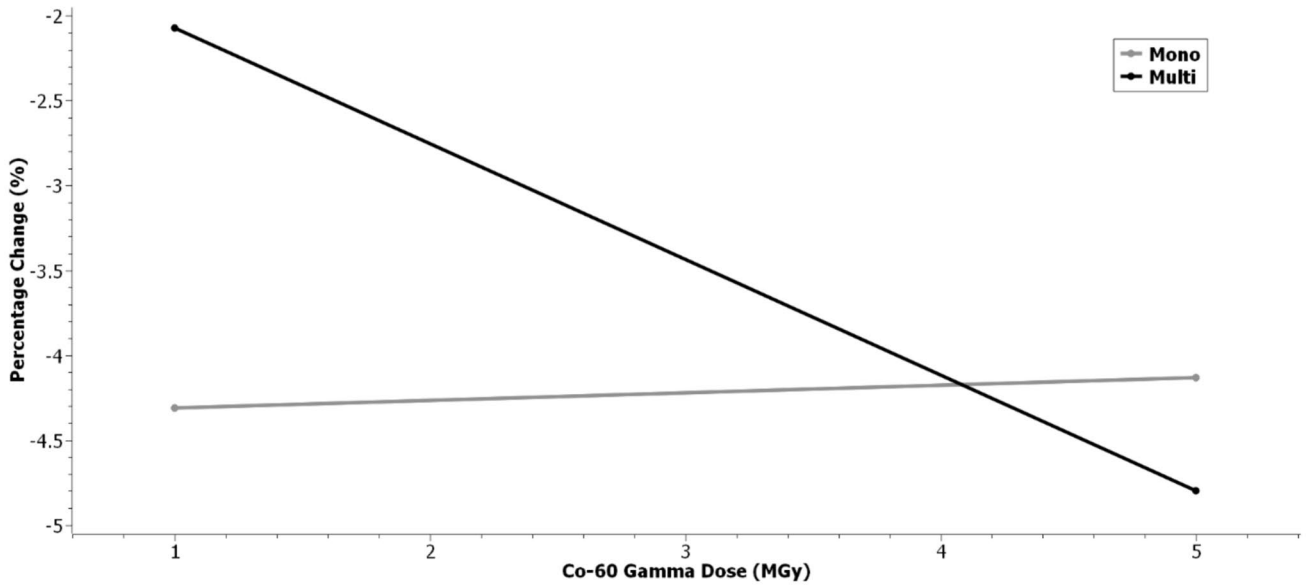

Fig. 12 Mean percentage change in magnetisation critical current density at 14 T for the mono- and multi-filamentary repeat samples post 1 and 5 MGy gamma irradiation – J_c values calculated at 20 K

The AC susceptibility profiles for the GdYBCO 7.5% Zr tape samples studied in [10] signalled a negligible T_c decrease but a large superconducting volume fraction decrease in the Cu-stabilised sample after 1 MGy gamma irradiation; this reduction in superconducting volume fraction was attributed to the gamma-induced increase in flux creep rate. In the GdYBCO 0% Zr Ag-only samples also studied in [10], J_c increased with gamma radiation dose up to 1 MGy, and this directly correlated with the decreases in flux creep rate; improved J_c is not associated with aging effects in YBCO or GdYBCO [27].

A better understanding of gamma irradiation and aging effects in combination is required. Gamma effects are present in the REBCO samples evaluated in this work (explained fully in Sect. 3.3), although the origin of inconsistencies in post-irradiation effects across the 5 MGy irradiated YBCO samples remains unknown.

3.2 GdYBCO Mono-filamentary Tape STEM and Origin of Gamma Effects

The noticeable difference in degree of J_c degradation between the YBCO mono-filamentary sample and the analogous GdYBCO Cu-stabilised sample analysed in [10] (designated as 'Cu-stabilised' sample in Fig. 13), post-irradiation to the same 1 MGy dose, sparked questions concerning the origin of gamma effects in REBCO tapes. The YBCO tape is more tolerant to gamma radiation than the GdYBCO tape, and the following STEM analysis inspired ideas for the theoretical origin of gamma effects in REBCO tapes. The proposed theoretical explanation in turn informed interpretation of the AC susceptibility profiles in Sect. 3.3 associated with the mono- and multi-filamentary YBCO sample J_c profiles included in Sect. 3.1.

Figure 14 shows HAADF-STEM images of the analogous mono-filamentary GdYBCO 15% Zr Ag-only tape samples before and after 1 MGy gamma irradiation. From magnetometry analysis on the Ag-only samples in [10], introduced microstructural damage was anticipated to consist of nm-scale amorphous zones caused by collision cascades, which should be easily detectable in STEM. This expectation was based on the observed enhanced J_c in the irradiated 0% Zr Ag-only samples without APCs, and greater J_c reduction in the APC-containing Ag-only samples relative to their Cu-stabilised counterparts (Fig. 13) [10]. The STEM images show no observable nm-scale amorphisation within the GdYBCO layer, the introduction of which would typically be necessary for J_c enhancement post-irradiation, and therefore do not provide evidence for gamma-induced changes to the microstructure.

If microstructural damage was not the cause of functionality changes in the GdYBCO samples, damage to the electronic structure was the next most plausible factor affecting performance because of the close connection between electronic structure and critical parameters [28]. Previously in literature, gamma rays have been known to cause changes to the REBCO electronic structure [15, 16]. Gamma radiation induces photoemission of core electrons in cuprate materials through incoherent Compton scattering, and released energetic Compton electrons are capable of further ionisation [29, 30]. Co-60 gamma rays are energetic enough to overcome the work function of core electrons in Gd and Y; Gd is

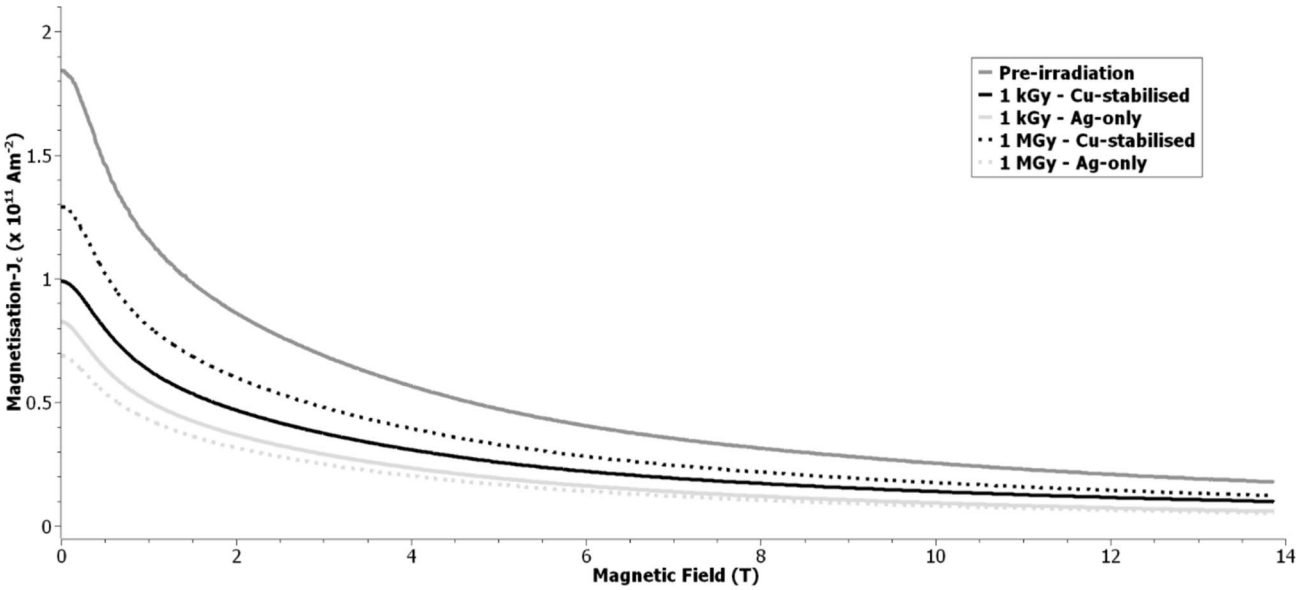

Fig. 13 Magnetisation critical current density versus magnetic field for the GdYBCO 15% Zr tape prior to gamma irradiation, and the Cu-stabilised and Ag-only samples after 1 kGy and 1 MGy gamma irradiation – J_c values calculated at 20 K [10]

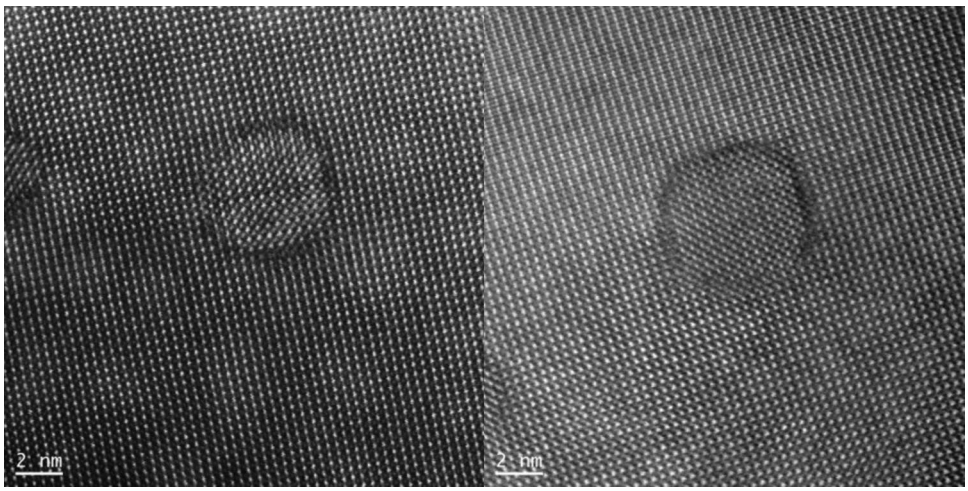

Fig. 14 HAADF-STEM images of GdYBCO 15% Zr Ag-only samples prior to (left) and post (right) 1 MGy gamma irradiation

a heavier element than Y, with a higher nuclear charge and thus core electron orbital energies (Gd 1 $s = 50{,}239$ eV and 2 $s = 8376$ eV; Y 1 $s = 17{,}038$ eV and 2 $s = 2373$ eV) [31]. Release of core electrons as photoelectrons could therefore explain radiation tolerance in GdYBCO versus YBCO tapes.

Figure 15 shows the AC susceptibility versus temperature profiles for the GdYBCO tape pre-/post-irradiation to 1 MGy. Gamma-induced decreases in superfluid density and superconducting volume fraction contributed to J_c degradation [10].

Superfluid density is composed of valence electrons [32], suggesting that in GdYBCO, release of likely Gd core electrons results in successive emission of Cu and O outer electrons. The lower energy of Y core electrons compared to Gd core electrons was suggested to be the determining factor improving radiation tolerance in the YBCO tape, and the justification behind this theory is discussed in Sect. 3.3. Higher levels of valence electron emission may also contribute to the greater reduction of J_c seen in the GdYBCO Ag-only samples compared to the Cu-stabilised samples (Figs. 13 and 15) [10]. Further study into the influence of aging effects on gamma-induced functionality changes in GdYBCO tape samples is necessary.

Separate studies involving electrical testing on REBCO tapes irradiated with low doses of gamma rays (on the order of kGy) did not demonstrate any loss of transport-J_c

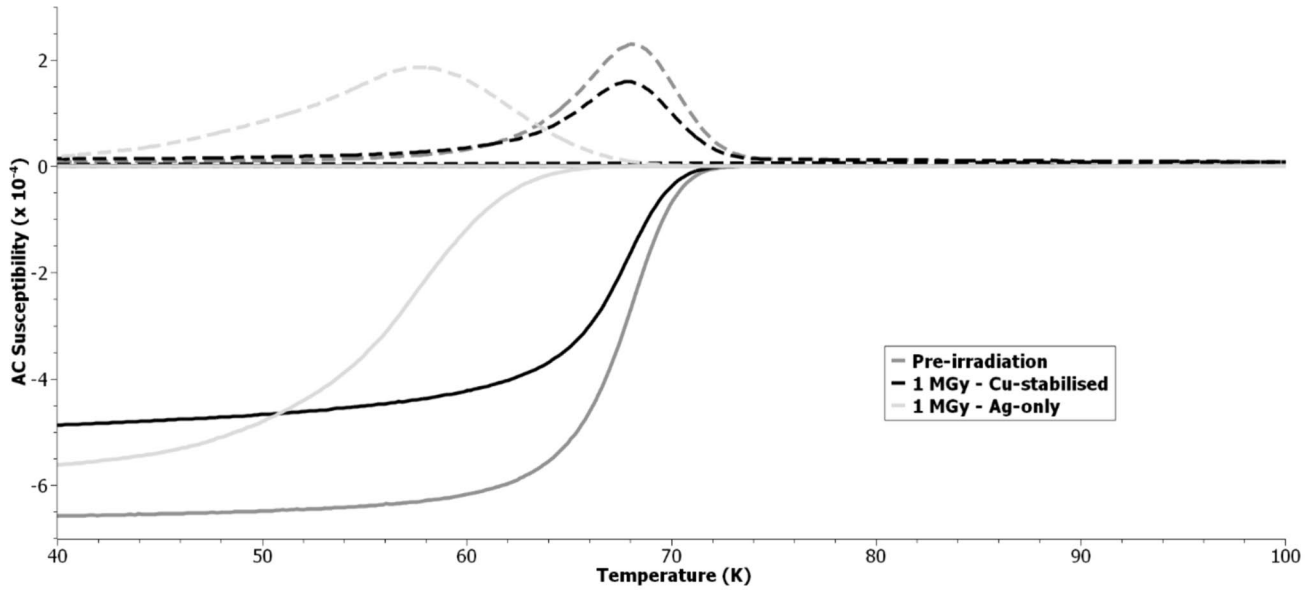

Fig. 15 AC susceptibility versus temperature for the GdYBCO 15% Zr tape prior to gamma irradiation, and the Cu-stabilised and Ag-only samples after 1 MGy gamma irradiation – susceptibility values at 14 T [10]

at 77 K under self-field nor at 4.2 K under applied fields [17, 18]; the introduction of microstructural damage in the form of Frenkel pair point defects (which are difficult to observe/resolve in STEM) with increasing radiation dose would typically result in a clear linear decrease in transport-J_c. As seen in [10] however, magnetisation-J_c in Cu-stabilised and/or APC-containing REBCO tapes did decrease because of 1 kGy gamma irradiation (Fig. 13).

It is possible that gamma-induced electronic structure changes in REBCO tapes are only observable using magnetometry methods, which unlike electrical measurements probe the flux-pinning landscape and magnetisation currents. This raised questions pertaining to the underlying mechanisms affecting surface screening currents but not bulk transport currents.

Incorporating learning outcomes from [10] into post-irradiation observations discussed in this work, it was inferred that changes in flux-pinning parameters, described by Ginzburg–Landau theory, can explain the effects of gamma irradiation on electronic behaviour [33].

Microstructural defects introduce local spatial variations in the superconducting order parameter (ψ), and this consequently reduces coherence length (ξ) and increases London penetration depth (λ_L) in the REBCO *ab*-axis with increasing radiation dose [34, 35]. Despite there being no evidence of gamma-induced microstructural damage in the GdYBCO Ag-only tape sample, in both [10] and this work, post-irradiation magnetic analysis was indicative of changes to ξ and λ_L.

Decreases in magnetisation-J_c, a direct calculation of screening current density, signifies an increase in λ_L [36, 37]. Normalised pinning force versus applied field profiles have been used to identify transitions in dominant pinning centre within the overall flux-pinning landscape and demonstrated that gamma rays alter ξ in REBCO tapes [10]. Both ξ and λ_L are related to ψ, therefore changes to these parameters indicates a higher rate of ψ spatial fluctuation [38].

Photoemission of core electrons as a result of gamma irradiation would lead to an increase in positive charge density through space. A greater overall positive charge density due to loss of core electrons may be akin to hole overdoping in cuprates, and could therefore cause suppression of ψ locally in REBCO tapes. In [10], gamma irradiation resulted in J_c degradation in all the GdYBCO Cu-stabilised and APC-containing samples (due to the decrease in superconducting volume fraction), yet enhancement of J_c in the Ag-only 0% Zr samples (attributed to reduced flux creep rate, i.e. improved flux-pinning); the YBCO tape samples in this work are Cu-stabilised and contain APCs. Increased spatial ψ modulation across the REBCO surface would explain the gamma-induced functionality changes observed in this work and in [10].

To further investigate gamma irradiation effects on the flux-pinning landscape in REBCO tapes, measurements of tunnelling conductance using a scanning tunnelling microscope (STM) could identify surface regions where ψ has been suppressed [39]. In future studies, STEM and positron annihilation lifetime spectroscopy (PALS) [40] could

be utilised for thorough analysis of these altered surface regions, which may aid in identification/confirmation of the underlying mechanisms causing functionality changes.

The conclusion from the observations discussed in this section is that gamma-induced changes to the flux-pinning landscape affect screening magnetisation current capability in the REBCO layer surface. Regardless of negligible effects on bulk transport current capability, this is still critical information for the qualification of REBCO tapes in tokamaks.

3.3 AC Losses

3.3.1 YBCO Mono-filamentary Tape

Section 3.2 explored the connections between magnetic measurement results and Ginzburg–Landau theoretical parameters. Understanding these connections informed interpretation of the following AC susceptibility measurement datasets, which in turn provided deeper insight into the gamma-induced changes to J_c discussed in Sect. 3.1.

AC susceptibility measurements probe superfluid density via T_c [41], superconducting volume fraction via diamagnetic saturation [42], and AC losses via the χ'' maximum value [24, 43]. In AC susceptibility profiles, superfluid density, AC losses and ψ spatial fluctuations are interconnected factors determining resultant superconducting volume fraction, and thus J_c.

As discussed in Sect. 3.1, there were inconsistencies in J_c degradation across the mono- and multi-filamentary repeat samples after gamma irradiation to a dose of 5 MGy. Therefore, objective comments on respective sample tolerance to the 5 MGy dose could not be made; the collected data on the 5 MGy irradiated samples is included in this work because it expands our knowledge of the connections between changes in different magnetic properties.

Figures 16 and 17 show the AC susceptibility versus temperature profile for 2 of the mono-filamentary repeat samples before and after irradiation to 1 MGy and 5 MGy, respectively. Reduction of superconducting volume fraction occurred without a decrease in superfluid density after irradiation to both gamma doses. This was in contrast to the previously studied GdYBCO tape samples (Fig. 15), where both superconducting volume fraction and superfluid density decreased as a consequence of increased ψ suppression, leading to greater J_c degradation relative to the YBCO analogue post-irradiation to the same dose. In the YBCO mono-filamentary tape samples, the degree of J_c degradation also decreased when dose was increased from 1 to 5 MGy. Without valence electron photoemission and subsequent changes to superfluid density, the resulting superconducting volume fractions in Figs. 16 and 17 reflected the degree of gamma-induced ψ spatial modulation and its effect on AC losses.

Figures 18 and 19 contain the pre-/post-irradiation calculated AC loss values for all 6 mono-filamentary samples after both doses, whilst Figs. 20 and 21 include the calculated percentage changes in AC loss.

After 1 MGy irradiation, AC losses increased in all 3 samples at 1 T, on average increased slightly at 7 T, and decreased in all 3 samples at 14 T. The calculated post-irradiation values correlate well with observed J_c changes at the same field strengths, and the decrease in AC loss with

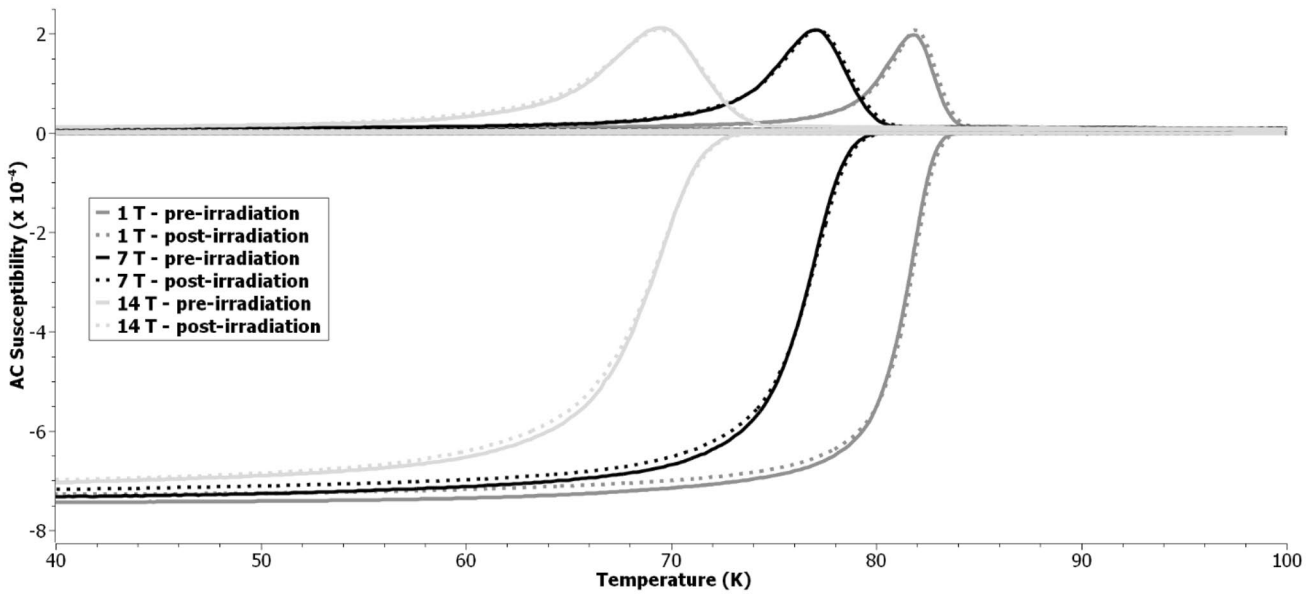

Fig. 16 AC susceptibility versus temperature for mono-filamentary repeat sample 3 prior to and post 1 MGy gamma irradiation—susceptibility values at 1, 7 and 14 T

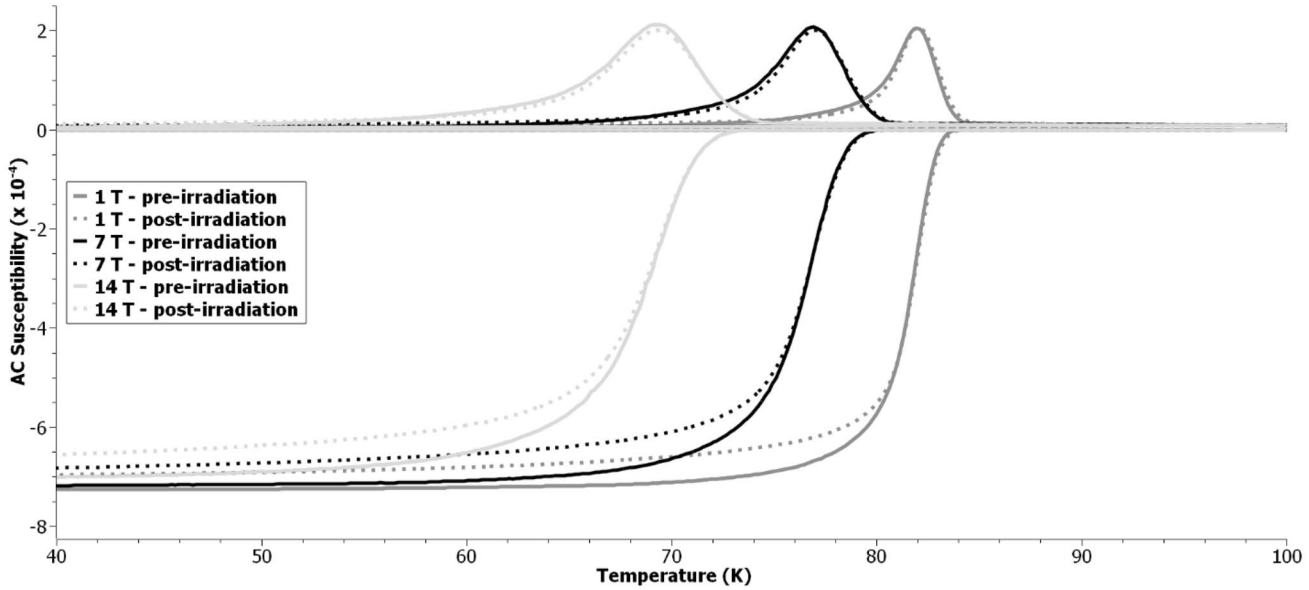

Fig. 17 AC susceptibility versus temperature for mono-filamentary repeat sample 3 prior to and post 5 MGy gamma irradiation—susceptibility values at 1, 7 and 14 T

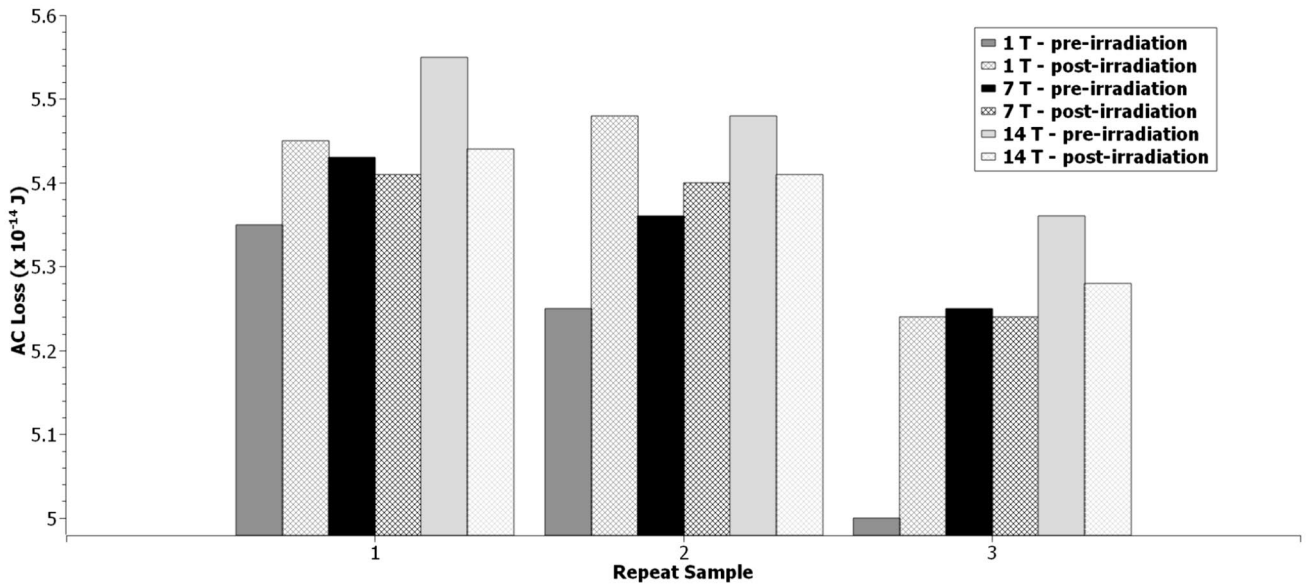

Fig. 18 Calculated AC loss values at 1, 7 and 14 T for the mono-filamentary repeat samples prior to and post 1 MGy gamma irradiation

increasing field likely contributed to maintenance of high superconducting volume fraction and J_c.

After 5 MGy irradiation, AC losses again increased in all 3 samples at 1 T, on average marginally increased at 7 T, and decreased in all 3 samples at 14 T. In repeat samples 1 and 2, AC losses increased in comparison to the 1 MGy irradiated samples, whilst in repeat sample 3 AC loss improved.

Across the mono-filamentary repeat samples, there was a direct correlation between level of J_c degradation and change to AC loss. When irradiated to 1 MGy, minimisation of AC loss enabled greater maintenance of J_c. After the 5 MGy dose, greater reduction of AC loss was instead coupled with lower post-irradiation J_c.

Gamma-induced AC loss changes also correlated well with variations in superconducting volume fraction observed in corresponding AC susceptibility profiles for each repeat sample (profiles included in Supplementary Information). Decreasing AC losses acted to either

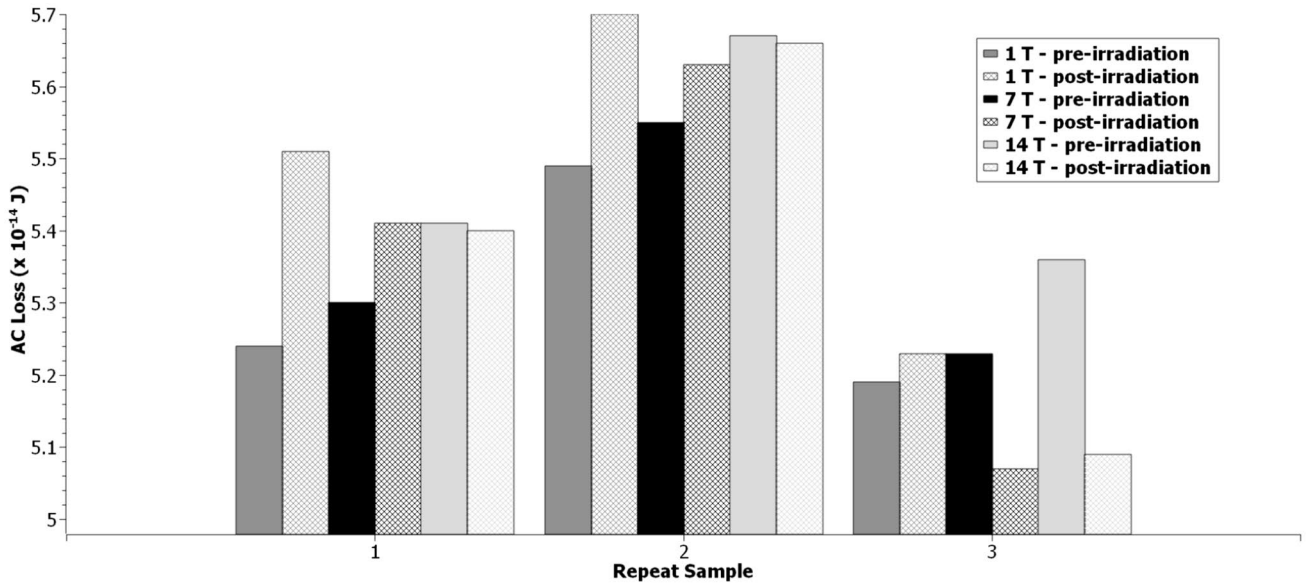

Fig. 19 Calculated AC loss values at 1, 7 and 14 T for the mono-filamentary repeat samples prior to and post 5 MGy gamma irradiation

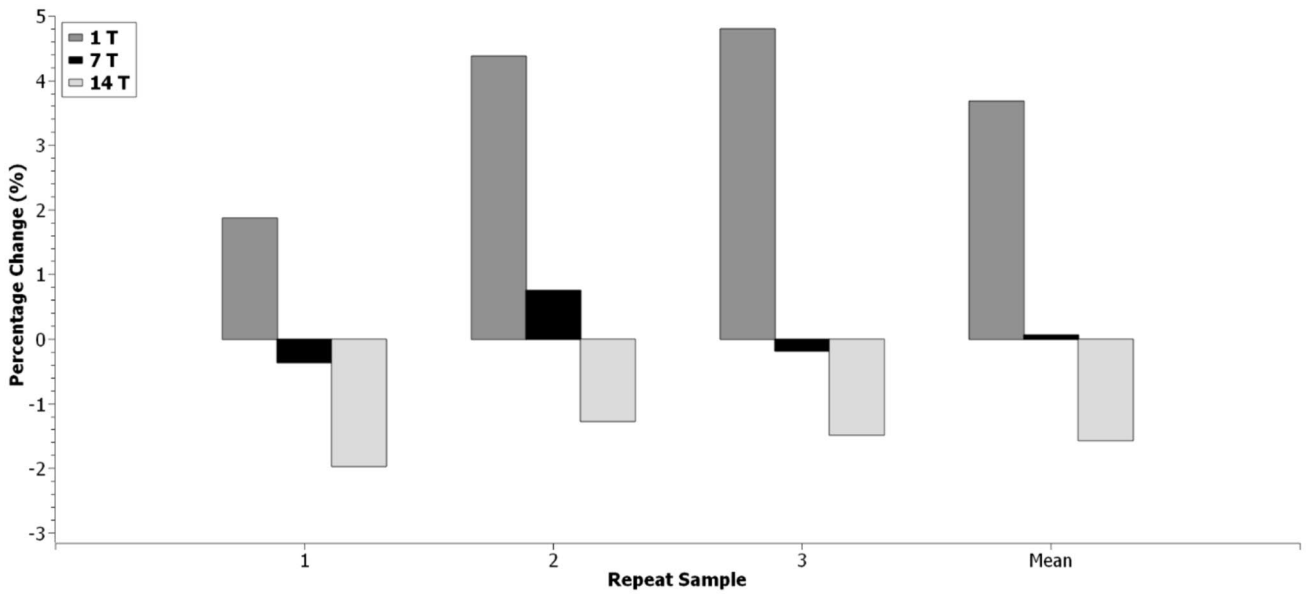

Fig. 20 Percentage change in AC losses at 1, 7 and 14 T for the mono-filamentary repeat samples post 1 MGy gamma irradiation

decrease or increase (increase at 14 T only) superconducting volume fraction after 1 MGy: in repeat sample 3, the decrease in superconducting volume fraction reducing with increasing field directly correlated to the improved AC loss and retention of J_c with increasing field. After 5 MGy, the largest decrease in AC loss was associated with the greatest decrease in superconducting volume fraction: in repeat sample 3, the increase in superconducting volume fraction reduction with increasing field was consistent with the decreased AC loss and retention of J_c with increasing field from 1 to 14 T.

Suppression of ψ through space reduced AC losses at 14 T after both gamma doses, but also noticeably reduced superconducting volume fraction in repeat sample 3 after 5 MGy (Figs. 17, 20 and 21). This was suggestive of a crossover occurring as disorder within the flux-pinning landscape increases, from improved retention of J_c due to decreases in AC loss after 1 MGy, to worsened

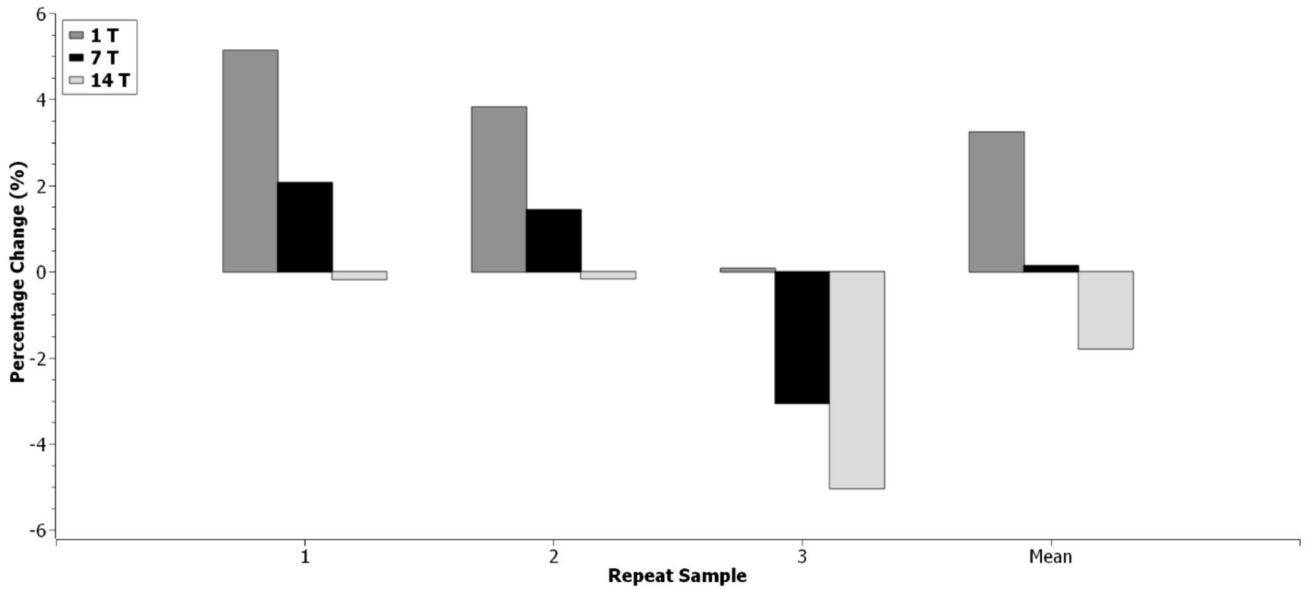

Fig. 21 Percentage change in AC losses at 1, 7 and 14 T for the mono-filamentary repeat samples post 5 MGy gamma irradiation

degradation associated with increasing disordered region volume and further reduction of AC loss after 5 MGy. Evolution of the pinning landscape was different in each repeat sample, some samples being more negatively affected by gamma radiation, and much greater variation in post-irradiation J_c was observed in the mono-filamentary samples after 5 MGy.

In the analogous GdYBCO Cu-stabilised samples investigated in [10], gamma irradiation increased flux creep rate under a DC 14 T field overall but increasing dose from 1 kGy to 1 MGy saw reduction of creep rate and improvement in J_c. In the YBCO mono-filamentary tape samples at 14 T with an AC drive field applied, enhanced maintenance of J_c was observed when the post-irradiation negative percentage change in AC loss decreased with increasing dose (as seen in the 5 MGy irradiated repeat samples 1 and 2). After 1 MGy irradiation, reduced AC loss was beneficial in the YBCO mono-filamentary samples, but post-irradiation to 5 MGy, a much greater loss of superconducting volume fraction because of heightened pinning landscape disorder corresponded to a perceived greater decrease in AC loss and was detrimental (as seen in the 5 MGy irradiated repeat sample 3).

From these two studies, it seems that the gamma-induced changes to the flux-pinning landscape associated with decreases in flux creep rate and increases in AC loss as dose is increased are desirable in APC-containing mono-filamentary tapes for retention of high J_c.

3.3.2 YBCO Multi-filamentary Tape

Figures 22 and 23 show the AC susceptibility versus temperature profile for 2 representative multi-filamentary repeat samples before/after irradiation to 1 MGy and 5 MGy, respectively. Again, reduction in superconducting volume fraction occurred without loss of superfluid density after irradiation to both gamma doses. In contrast to the mono-filamentary samples, there was a greater decrease in J_c as dose increased from 1 to 5 MGy in the multi-filamentary samples, and this was associated with changes in AC loss as a result of increased spatial ψ modulation within the flux-pinning landscape.

Figures 24 and 25 contain the pre-/post-irradiation calculated AC loss values for all 6 multi-filamentary samples after both doses, whilst Figs. 26 and 27 include the calculated percentage changes in AC loss.

After 1 MGy irradiation, AC losses decreased in all 3 samples at 1 T and 7 T, and on average decreased at 14 T, with AC loss in 1 sample marginally increasing. The calculated post-irradiation values correlate well with observed J_c changes at the same field strengths.

After 5 MGy irradiation, AC losses decreased in all 3 samples at each measured field. Greater mean decreases in AC loss were observed across all 3 measured fields relative to the 1 MGy irradiated samples, and the mean percentage decrease in AC loss increased with field. On average, AC loss and J_c decreased more when the gamma dose was

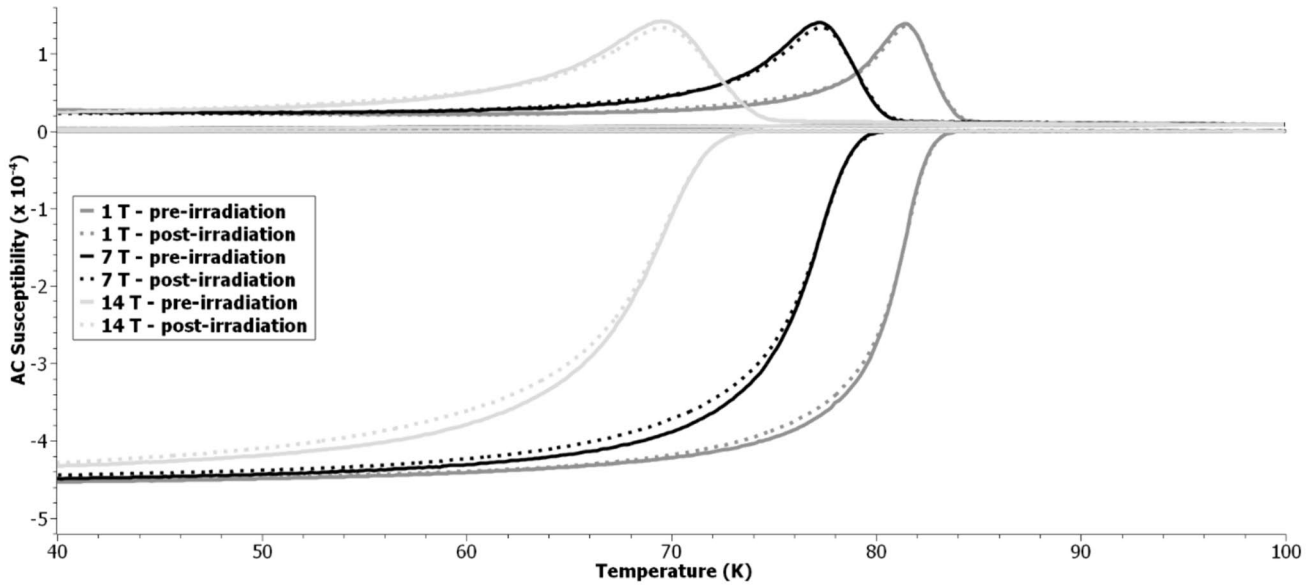

Fig. 22 AC susceptibility versus temperature for multi-filamentary repeat sample 3 prior to and post 1 MGy gamma irradiation—susceptibility values at 1, 7 and 14 T

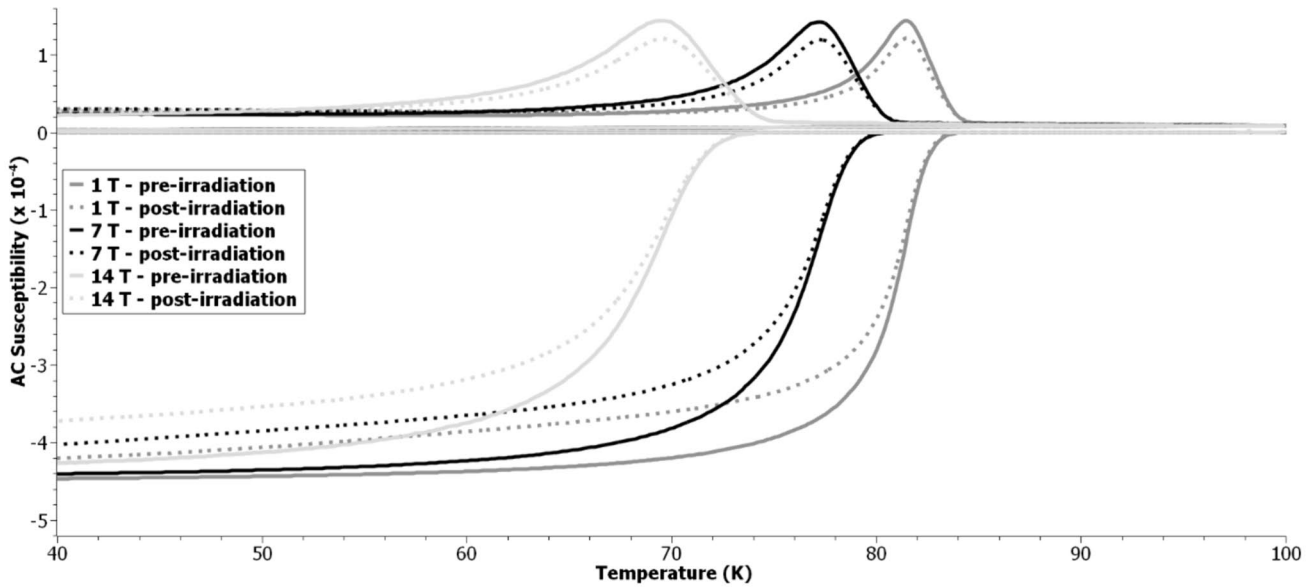

Fig. 23 AC susceptibility versus temperature for multi-filamentary repeat sample 2 prior to and post 5 MGy gamma irradiation—susceptibility values at 1, 7 and 14 T

increased from 1 to 5 MGy in the multi-filamentary samples (Figs. 12 and 28).

As seen in the mono-filamentary repeat samples, there was a direct correlation between level of J_c degradation and change to AC loss across all the multi-filamentary repeat samples. For both gamma doses, a greater decrease in AC loss corresponded to lower J_c. J_c reduction after irradiation was attributed to increased suppression of ψ through space, whilst the striations present minimised AC losses even further relative to the mono-filamentary samples. Though the striations improved retention of J_c in the multi-filamentary samples after 1 MGy, after 5 MGy the thinner filaments were then more susceptible to J_c degradation.

Gamma-induced AC loss changes also correlated well with variations in superconducting volume fraction observed in associated AC susceptibility profiles for each repeat sample (profiles included in Supplementary Information). Decreasing AC losses acted to either decrease or increase

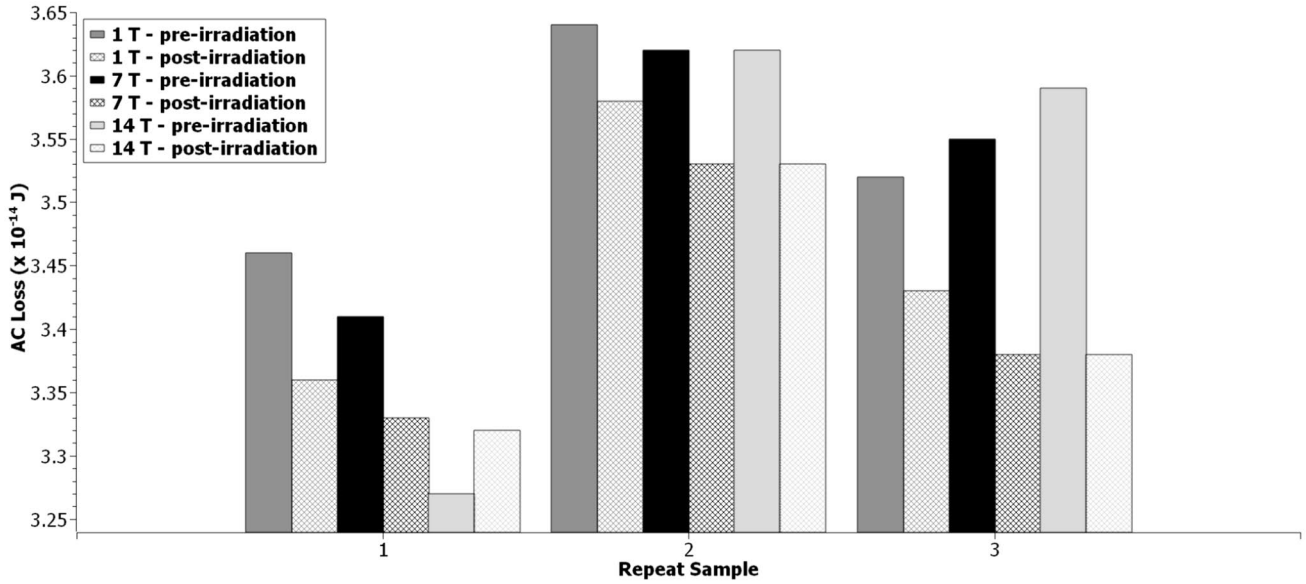

Fig. 24 Calculated AC loss values at 1, 7 and 14 T for the multi-filamentary repeat samples prior to and post 1 MGy gamma irradiation

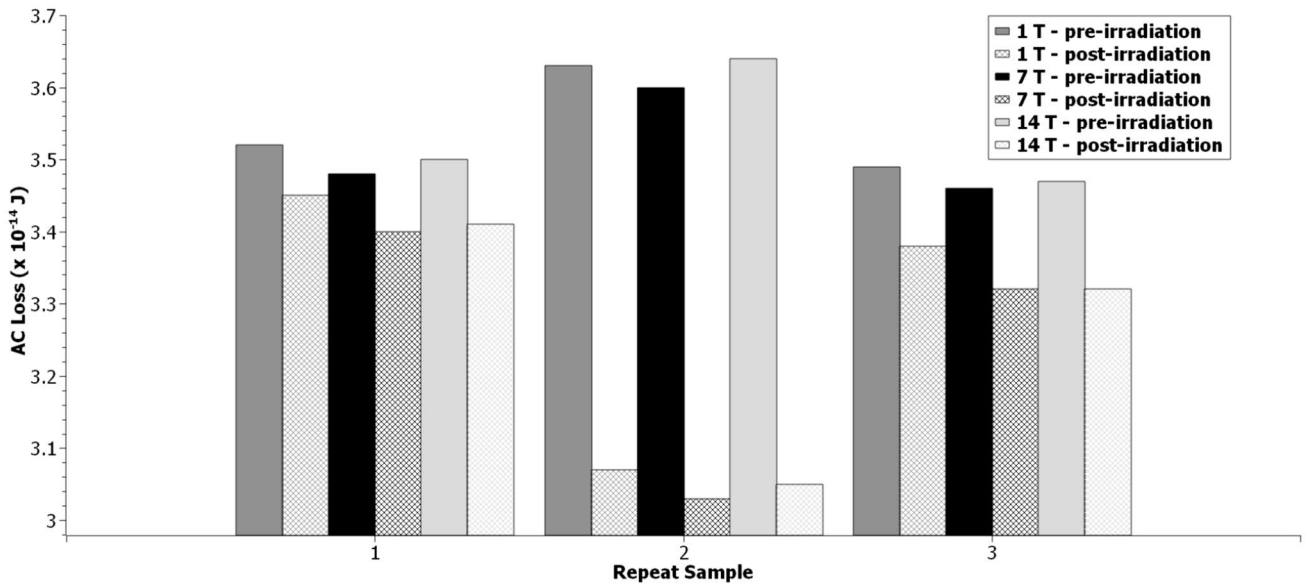

Fig. 25 Calculated AC loss values at 1, 7 and 14 T for the multi-filamentary repeat samples prior to and post 5 MGy gamma irradiation

(increase at 7 and 14 T only) superconducting volume fraction after 1 MGy, whilst the highest decrease in AC loss was associated with the highest decrease in superconducting volume fraction after 5 MGy. Interestingly, in the 1 MGy irradiated repeat sample 1, the increase in AC loss at 14 T was associated with a sizable increase in superconducting volume fraction, which corresponded to greater retention of J_c at 14 T relative to 1 and 7 T (and to repeat samples 2 and 3 at 14 T).

Local suppression of ψ reduced AC losses after both gamma doses, but also noticeably reduced superconducting volume fraction in repeat sample 2 after 5 MGy (Figs. 23, 26 and 27). These similar patterns supported the introduced idea of a crossover occurring with increasing dose, from beneficial increases in pinning landscape disorder improving J_c maintenance, to detrimental loss of superconducting volume fraction as a result of further increases in disorder, as discussed in Sect. 3.3.1. The more dramatic transition from retention

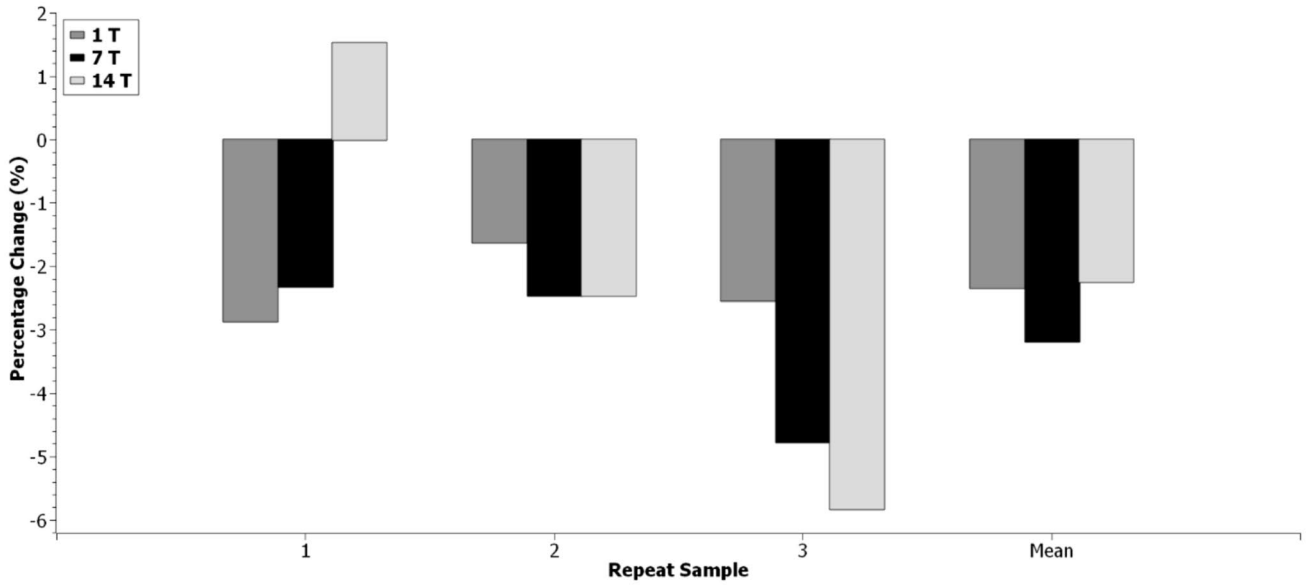

Fig. 26 Percentage change in AC losses at 1, 7 and 14 T for the multi-filamentary repeat samples post 1 MGy gamma irradiation

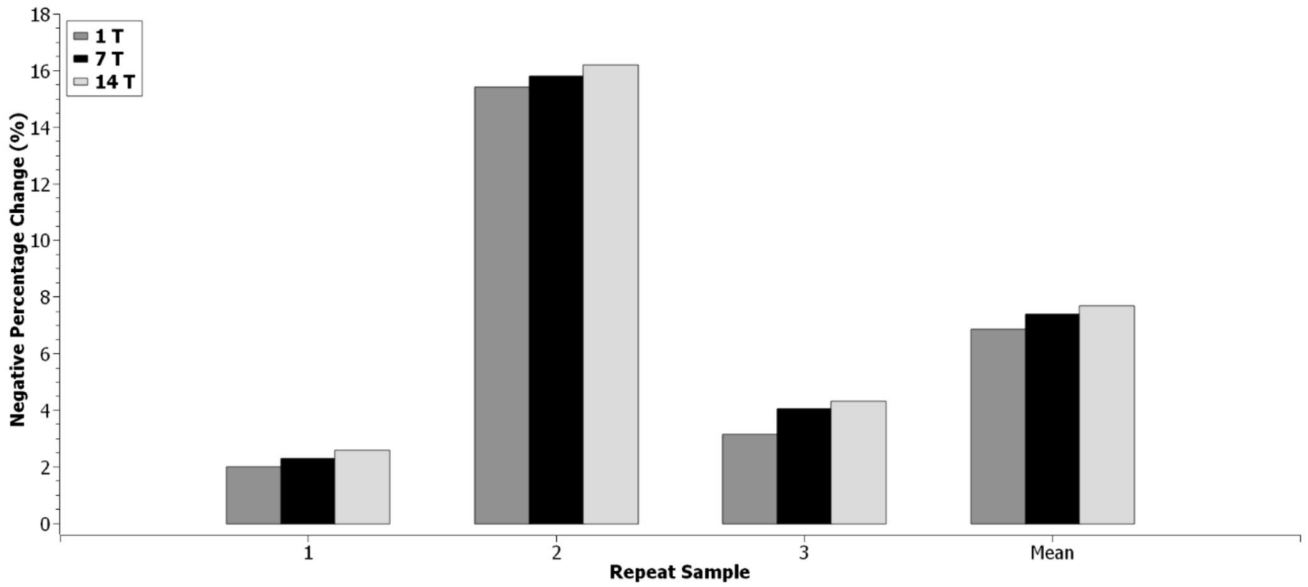

Fig. 27 Percentage change in AC losses at 1, 7 and 14 T for the multi-filamentary repeat samples post 5 MGy gamma irradiation

of J_c to degradation of performance in the multi-filamentary samples was probably due to the higher post-irradiation ratio of disordered region volume to optimally superconducting region volume within the individual filaments. Evolution of the flux-pinning landscape was again different in each multi-filamentary repeat sample, some samples being more negatively affected by gamma radiation, and much greater variation in post-irradiation J_c was observed after 5 MGy.

Overall, AC losses decreased in both the mono- (at 14 T) and multi-filamentary tape samples post-irradiation with gamma rays. Minimisation of AC loss relative to the mono-filamentary samples improved maintenance of J_c in the multi-filamentary samples after 1 MGy irradiation, though a higher level of disorder within the flux-pinning landscape was associated with increased J_c degradation after 5 MGy.

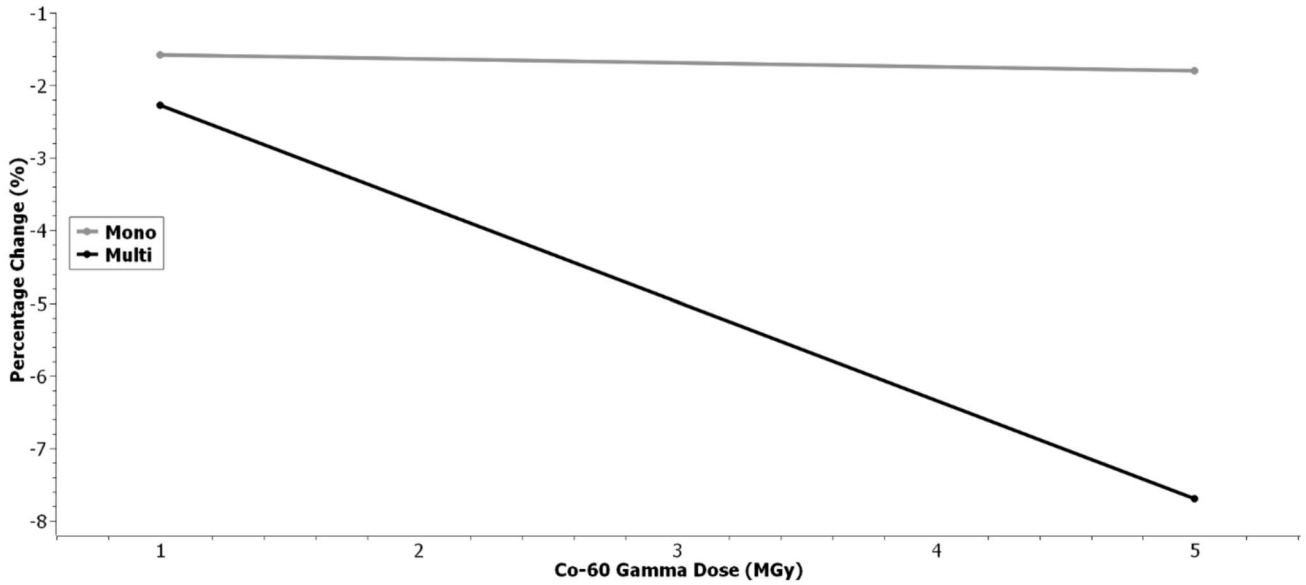

Fig. 28 Mean percentage change in AC losses at 14 T for the mono- and multi-filamentary repeat samples post 1 and 5 MGy gamma irradiation

4 Conclusion

The primary conclusions from this work were that reduction in AC losses improved retention of magnetisation-J_c in the YBCO multi-filamentary tape samples compared with the YBCO mono-filamentary samples after 1 MGy gamma irradiation, however, when the dose was increased to 5 MGy, on average the multi-filamentary samples were more prone to J_c degradation. These observations were attributed to the striations and smaller filament width present within the multi-filamentary tape. The thinner filament cross-section minimised AC loss, but consequently resulted in a higher mean post-irradiation ratio of disordered region volume to optimally superconducting region volume within the individual filaments after the 5 MGy dose.

STEM did not indicate the presence of gamma-induced microstructural damage within the GdYBCO layer of an analogous mono-filamentary tape. In the absence of observable nm-scale amorphisation, photoemission of core electrons out of the REBCO layer surface was suggested as a potential theoretical explanation behind the observed gamma irradiation effects. Connections made between post-irradiation magnetometry analysis and Ginzburg–Landau theoretical parameters implied that gamma rays were locally suppressing ψ across the REBCO layer surface through hole overdoping, increasing disorder within the flux-pinning landscape.

Gamma radiation alters λ_L and ξ, demonstrated previously by changes to magnetisation-J_c and in dominant pinning centre [10, 36, 37]. Both ξ and λ_L are related to ψ, thus gamma-induced changes to these parameters would have a knock-on effect, leading to heightened ψ spatial fluctuations [38]. In APC-containing REBCO tapes such as the YBCO and GdYBCO samples investigated in this work, increasing ψ modulation with radiation dose is known to cause performance degradation [10, 44].

The proposed release of core electrons as photoelectrons had a much weaker effect on J_c and T_c than introduced microstructural damage in REBCO tapes [45]. Considering the potential impact of local ψ suppression versus local ψ transitions to zero on the flux-pinning landscape in APC-containing tapes, less prominent degradation as a result of photoemission was expected. However, similar to patterns observed as microstructural damage increases in REBCO tapes (under high fields) [44], there is also a crossover with increasing gamma dose, from introduction of beneficial increases in pinning landscape disorder reducing AC losses for improved maintenance of J_c, to more rapid degradation as superconducting volume fraction decreases with higher levels of disorder. The transition to degradation was more apparent in the multi-filamentary samples.

The degree of degradation caused by emission of core electron photoelectrons, thus gamma radiation tolerance in REBCO tapes, appeared to be dependent on the atomic number of the rare-earth element, with heavier elements having higher probabilities of released core electrons triggering further emission of Cu/O valence electrons. In contrast to the previously examined GdYBCO tapes [10], T_c did not change in any YBCO sample included in this work post-irradiation, indicating that valence electron superfluid density was unaffected by Co-60 gamma rays, which likely contributed to the higher retention of J_c after irradiation to the same 1 MGy dose.

Gamma-induced ψ fluctuations without T_c reduction may be a consequence of core electron photoemission causing the positive charge (hole) buildup in YBCO, as opposed to the valence electron density changes that are introduced with dopants.

In summary, this work provides critical information regarding gamma-induced changes to surface screening current capability in REBCO tapes, and evidence for consideration of gamma and neutron effects in tandem being necessary for tokamak magnet material qualification studies. For a full understanding of performance evolution under gamma and neutron irradiation, complementary magnetic and electrical testing will be required. Future qualification studies should explore gamma irradiation effects further, particularly at higher doses > 1 MGy where larger differences in post-irradiation J_c and AC losses were observed. STM measurements of tunnelling conductance combined with use of techniques such as STEM and PALS would be beneficial for identification/confirmation of the definitive microscopic physical mechanism causing gamma-induced magnetic property changes in REBCO tapes. Further investigation into the influence of aging effects on gamma-induced functionality changes in REBCO tapes would also be of benefit.

Supplementary Information The online version contains supplementary material available at https://doi.org/10.1007/s10948-024-06808-4.

Acknowledgements This work has been part-funded by the EPSRC Energy Programme [grant number EP/W006839/1]. To obtain further information on the data and models underlying this paper please contact PublicationsManager@ukaea.uk. For the purpose of open access, the authors have applied a Creative Commons Attribution (CC BY) licence (where permitted by UKRI, 'Open Government Licence' or 'Creative Commons Attribution No-derivatives (CC BY-ND) licence' may be stated instead) to any Author Accepted Manuscript version arising. We acknowledge the support of The University of Manchester's Dalton Cumbrian Facility (DCF), a partner in the National Nuclear User Facility, the EPSRC UK National Ion Beam Centre and the Henry Royce Institute. We recognise R. Edge for their assistance during the gamma irradiation experiments. The research used UKAEA's Materials Research Facility, which has been funded by and is part of the UK's National Nuclear User Facility and Henry Royce Institute for Advanced Materials.

Author Contribution H.J.C. conducted all magnetic analysis and wrote the main manuscript text. H.S. conducted scanning transmission electron microscopy analysis. Y.Z. was responsible for preparation of the YBCO and GdYBCO coated conductor tape samples. All authors reviewed the manuscript.

Data Availability Data that support the findings of this study is provided within the main manuscript and included supplementary information.

Declarations

Competing Interest The authors declare no competing interests.

References

1. Bruzzone, P., Fietz, W.H., Minervini, J.V., Novikov, M., Yanagi, N., Zhai, Y., Zheng, J.: High temperature superconductors for fusion magnets. Nucl. Fusion **58**(10), 103001 (2018)
2. Lee, T.S., Jenkins, I., Surrey, E., Hampshire, D.P.: Optimal design of a toroidal field magnet system and cost of electricity implications for a tokamak using high temperature superconductors. Fusion Eng. Des. **98–99**, 1072–1075 (2015)
3. Grilli, F., Kario, A.: How filaments can reduce AC losses in HTS coated conductors: a review. Supercond. Sci. Technol. **29**, 083002 (2016)
4. Zhang, H., Wen, Z., Grilli, F., Gyftakis, K., Mueller, M.: Alternating Current Loss of Superconductors Applied to Superconducting Electrical Machines. Energies **14**(8), 2234 (2021)
5. Pekarcikova, M., Frolek, L., Necpal, M., Cuninkova, E., Skarba, M., Hulacova, S., Ferencik, F., Bocakova, B.: Optimization of REBCO Tapes through Division and Striation for Use in Superconducting Cables with Low AC Losses. Materials **16**, 7333 (2023)
6. Wulff, A.C., Abrahamsen, A.B., Insinga, A.R.: Multifilamentary coated conductors for ultra-high magnetic field applications. Supercond. Sci. Technol. **34**, 053003 (2021)
7. Vojenciak, M., Kario, A., Ringsdorf, B., Nast, R., van der Laan, D.C., Scheiter, J., Jung, A., Runtsch, B., Gomory, F., Goldacker, W.: Magnetization ac loss reduction in HTS CORC® cables made of striated coated conductors. Supercond. Sci. Technol. **28**, 104006 (2015)
8. Brandt, E.H., Indenbom, M.: Type-II-superconductor strip with current in a perpendicular magnetic field. Phys. Rev. B **48**, 12893 (1993)
9. Zeldov, E., Clem, J.R., McElfresh, M., Darwin, M.: Magnetization and transport currents in thin superconducting films. Phys. Rev. B **49**, 9802 (1994)
10. Campbell, H.J., Zhang, Y., Fukushima, T.: Probing Evolution of the Flux-Pinning Landscape in REBCO Coated Conductors Caused by Gamma Irradiation Using DC and AC Magnetometry: A Novel Approach to Tokamak Magnet Material Development. J. Supercond. Novel Magn. **37**, 41 (2024)
11. Sumption, M.D., Murphy, J.P., Haugan, T., Majoros, M., van der Laan, D.C., Long, N., Collings, E.W.: AC losses of Roebel and CORC® cables at higher AC magnetic fields and ramp rates. Supercond. Sci. Technol. **35**, 025006 (2022)
12. Windsor, C.G., Morgan, J.G.: Neutron and gamma flux distributions and their implications for radiation damage in the shielded superconducting core of a fusion power plant. Nucl. Fusion **57**, 116032 (2017)

13. Leyva, A., Mora, M., Martin, G., Martinez, A.: Irradiation effects of Co-60 gamma rays in YBCO thick films. Supercond. Sci. Technol. **8**, 816 (1995)
14. Akduran, N.: Gamma irradiation effects on $EuBa_2Cu_3O_7$ high temperature superconductor. Radiat. Phys. Chem. **83**, 61–66 (2013)
15. Kutsukake, T., Somei, H., Ohki, Y., Nagasawa, K., Kaneko, F.: Gamma-Irradiation Effect on High-T_c Superconductor $YBa_2Cu_3O_{7-x}$. Jap. J. Appl. Phys. **28**(Part 2, No. 8), L1393 (1989)
16. El-Hamalawy, A.A.E.-S., El-Zaidia, M.M., Ghali, E.A.: The Effects of Gamma-Radiation on the High T_c Superconductors $Er_1Ba_2Cu_3O_{7-\delta}$. Jap. J. Appl. Phys. **31**(Part 1, No. 11), 3529 (1992)
17. Chislett-McDonald, S.B.L., Bullock, L., Turner, A., Schoofs, F., Dieudonne, Y., Reilly, A.: In-situ critical current measurements of REBCO coated conductors during gamma irradiation. Supercond. Sci. Technol. **36**, 095019 (2023)
18. Taheri, B., Pinto, V., Cemmi, A., Di Sarcina, I., Scifo, J., Masi, A., Verna, A., Celentano, G.: Sensitivity of REBCO Tapes and Thin Film to γ-Irradiation. IEEE Trans. Appl. Supercond. **34**(5), 6600105 (2024)
19. Nikolo, M.: Flux dynamics in high-temperature superconductors. Supercond. Sci. Technol. **6**, 618 (1993)
20. Amemiya, N., Tominaga, N., Toyomoto, R., Nishimoto, T., Sogabe, Y., Yamano, S., Sakamoto, H.: Coupling time constants of striated and copper-plated coated conductors and the potential of striation to reduce shielding current-induced fields in pancake coils. Supercond. Sci. Technol. **31**, 025007 (2018)
21. Amemiya, N., Shigemasa, M., Takahashi, A., Wang, N., Sogabe, Y., Yamano, S., Sakamoto, H.: Effective reduction of magnetisation losses in copper-plated multifilament coated conductors using spiral geometry. Supercond. Sci. Technol. **35**, 025003 (2022)
22. Superpower Furukawa, Superpower 2G HTS Coated Conductors. www.superpower-inc.com/content/2g-hts-wire (2013)
23. Eisterer, M., Fuger, R., Chudy, M., Hengstberger, F., Weber, H.W.: Neutron irradiation of coated conductors. Supercond. Sci. Technol. **23**(1), 014009 (2009)
24. Seo, S., Noh, H., Li, N., Jiang, J., Tarantini, C., Shi, R., Jung, S., Oh, M. J., Liu, M., Lee J., Gu, G., Jung Jo, Y., Park, T., Hellstrom, E. E., Gao, P., Lee, S.: Artificially engineered nanostrain in $FeSe_xTe_{1-x}$ superconductor thin films for supercurrent enhancement. NPG Asia Mater. **12**(7), (2020)
25. Jung, S., Han, Y., Kim, J.H., Hidayati, R., Rhyee, J., Lee, J.M., Kang, W.N., Choi, W.S., Jeon, H., Suk, J., Park, T.: High critical current density and high-tolerance superconductivity in high-entropy alloy thin films. Nat. Commun. **13**, 3373 (2022)
26. Gomory, F., Vojenciak, M., Solovyov, M., Frolek, L., Souc, J., Seiler, E., Bauer, M., Falter. M.: AC susceptibility as a characterization tool for coated conductor tapes. Superconductor Science and Technology **30**, 114001 (2017)
27. Schlesier, K., Huhtinen, H., Granroth, S., Paturi, P.: An aging effect and its origin in GdBCO thin films. J. Phys. Conf. Ser. **234**, 012036 (2010)
28. Phillips, J.C.: Percolative theories of strongly disordered ceramic high-temperature superconductors. Proc. Natl. Acad. Sci. **107**(4), 1307 (2010)
29. Zhao, X., Yu, J., Wang, Y., Yu, G., Chen, Y., Zhang, Z.: Radiation effects on the T_c of Bi-system superconductors by proton and gamma irradiation. Physica C **337**(1), 234–238 (2000)
30. Tolpygo, S.K., Lin, J., Gurvitch, M., Hou, S., Phillips, J.M.: Effect of oxygen defects on transport properties and T_c of $YBa_2Cu_3O_{6+x}$: Displacement energy for plane and chain oxygen and implications for irradiation-induced resistivity and T_c suppression. Phys. Rev. B **53**, 12462 (1996)
31. Lawrence Berkley National Laboratory, X-Ray Data Booklet Section 1.1 electron binding energies. (2009). https://xdb.lbl.gov/Section1/Sec_1-1.html
32. Attfield, J.P.: Chemistry and high temperature superconductivity. J. Mater. Chem. **21**, 4756 (2011)
33. Ginzburg, V.L., Landau, L.D: On the Theory of Superconductivity. In: On Superconductivity and Superfluidity. Springer, Berlin, Heidelberg. (2009). https://doi.org/10.1007/978-3-540-68008-6_4
34. Choi, W.J., Ahmad, D., Seo, Y.I., Ko, R.K., Kwon, Y.S.: Effect of the proton irradiation on the thermally activated flux flow in superconducting SmBCO coated conductors. Sci. Rep. **10**(1), 2017 (2020)
35. Eley, S., Leroux, M., Rupich, M.W., Miller, D.J., Sheng, H., Niraula, P.M., Kayani, A., Welp, U., Kwok, W.K., Civale, L.: Decoupling and tuning competing effects of different types of defects on flux creep in irradiated $YBa_2Cu_3O_{7-\delta}$ coated conductors. Supercond. Sci. Technol. **30**(1), 015010 (2016)
36. Sarma, G.: On the influence of a uniform exchange field acting on the spins of the conduction electrons in a superconductor. J. Phys. Chem. Solids **24**, 1029 (1963)
37. Maki, K., Tsuneto, T.: Pauli paramagnetism and superconducting state. Progress Theoret. Phys. **31**, 945 (1964)
38. Kwok, W.-K., Welp, U., Glatz, A., Koshelev, A.E., Kihlstrom, K.J., Crabtree, G.W.: Vortices in high-performance high-temperature superconductors. Rep. Prog. Phys. **79**(11), 116501 (2016)
39. Fente, A., Meier, W.R., Kong, T., Kogan, V.G., Bud'ko, S.L., Canfield, P.C., Guillamon, I., Suderow, H.: Influence of multiband sign-changing superconductivity on vortex cores and vortex pinning in stoichiometric high-T_c $CaKFe_4As_4$. Phys. Rev. B. **97**, 134501 (2018)
40. Chudy, M., Eisterer, M., Weber, H.W., Veterníková, J., Sojak, S., Slugeň, V.: Point defects in YBa2Cu3O7−x studied using positron annihilation. Supercond. Sci. Technol. **25**(7), 075017 (2012)
41. Uemura, Y.J., Luke, G.M., Sternlieb, B.J., Brewer, J.H., Carolan, J.F., Hardy, W.N., Kadono, R., Kempton, J.R., Kiefl, R.F., Kreitzman, S.R., Mulhern, P., Riseman, T.M., Williams, D.L., Yang, B.X., Uchida, S., Takagi, H., Gopalakrishnan, J., Sleight, A.W., Subramanian, M.A., Chien, C.L., Cieplak, M.Z., Xiao, G., Lee, V.Y., Statt, B.W., Stronach, C.E., Kossler, W.J., Yu, X.H.: Universal correlations between T_c and n_s/m^* (carrier density over effective mass) in high T_c cuprate superconductors. Phys. Rev. Lett. **62**(19), 2317 (1989)
42. Srinivas, G., Howard, C.A., Bennington, S.M., Skipper, N.T., Ellerby, M.: Effect of hydrogenation on structure and superconducting properties of CaC_6. J. Mater. Chem. **19**, 5239 (2009)
43. Anderson, P.W., Kim, Y.B.: Hard superconductivity: theory of the motion of Abrikosov flux lines. Rev. Mod. Phys. **36**, 39 (1964)
44. Fischer, D.X., Prokopec, R., Emhofer, J., Eisterer, M.: The effect of fast neutron irradiation on the superconducting properties of REBCO coated conductors with and without artificial pinning centers. Supercond. Sci. Technol. **31**(4), 044006 (2018)
45. Prokopec, R., Fischer, D.X., Weber, H.W., Eisterer, M.: Suitability of coated conductors for fusion magnets in view of their radiation response. Supercond. Sci. Technol. **28**(1), 014005 (2014)